Entergy

Entergy Operations, Inc.
1340 Echelon Parkway
Jackson, MS 39213-8298
Tel 601 368 5758

Michael A. Krupa
Director
Nuclear Safety & Licensing

CNRO-2002-00058

December 16, 2002

U. S. Nuclear Regulatory Commission
Attn.: Document Control Desk
Washington, DC 20555-0001

SUBJECT: Entergy Operations, Inc.
Proposed Alternative to ASME Examination Requirements for Repairs Performed on Reactor Vessel Head Penetrations

Arkansas Nuclear One, Unit 1
Docket No. 50-313
License No. DPR-51

REFERENCES:

1. Entergy Operations, Inc. Letter No. CNRO-2002-00054 to the NRC, "Proposed Alternative to ASME Examination Requirements for Repairs Performed on Reactor Vessel Head Penetrations," dated November 26, 2002

2. Entergy Operations, Inc. Letter No. CNRO-2002-00052 to the NRC, "Proposed Alternative to ASME Examination Requirements for Repairs Performed on Reactor Vessel Head Penetrations," dated October 28, 2002

Dear Sir or Madam:

In Reference 1, Entergy Operations, Inc. (Entergy) provided to the NRC staff four calculations performed by Framatome-ANP that supported Relief Request Nos. ANO1-R&R-003, Rev. 0 and ANO1-R&R-004, Rev. 0, which were submitted via Reference 2. As documented in Reference 1, Framatome-ANP considers information contained in Framatome Documents 32-5021538 and 32-5021539 (ANO Calculations 86-E-0074-156 and 86-E-0074-161) to be proprietary and confidential pursuant to 10 CFR 2.790(a)(4) and 10 CFR 9.17(a)(4).

In Reference 1, Entergy stated we would provide nonproprietary versions of the Framatome documents when they became available. This letter transmits those nonproprietary versions as Enclosures 1 and 2.

A047

Should you have any questions regarding this letter, please contact Guy Davant at (601) 368-5756.

This letter contains no commitments.

Very truly yours,

M. A. Krupa

MAK/GHD/bal

Enclosures:
1. Framatome Document 32-5021538 (ANO Calculation 86-E-0074-156)
2. Framatome Document 32-5021539 (ANO Calculation 86-E-0074-161)

cc:
Mr. C. G. Anderson (ANO) (w/o)
Mr. W. R. Campbell (ECH) (w/o)
Mr. G. A. Williams (ECH) (w/o)

Mr. T. W. Alexion, NRR Project Manager (ANO-2)
Mr. R. L. Bywater, NRC Senior Resident Inspector (ANO) (w/o)
Mr. E. W. Merschoff, NRC Region IV Regional Administrator (w/o)
Mr. W. D. Reckley, NRR Project Manager (ANO-1)

ENCLOSURE 1

CNRO-2002-00058

FRAMATOME DOCUMENT 32-5021538
(ANO CALCULATION 86-E-0074-156)

FRAMATOME ANP

CALCULATION SUMMARY SHEET (CSS)

Document Identifier 32 - 5021538 - 01

Title ANO-1 CRDM NOZZLE IDTB J-GROOVE WELD FLAW EVALUATION

PREPARED BY:		REVIEWED BY:	
		METHOD. ☒ DETAILED CHECK ☐ INDEPENDENT CALCULATION	
NAME D.E. KILLIAN		NAME A.D. NANA	
SIGNATURE		SIGNATURE	
TITLE ADVISORY ENGR.	DATE 12/9/02	TITLE PRINCIPAL ENGR.	DATE 12/9/02
COST CENTER 41026	REF. PAGE(S) 37	TM STATEMENT: REVIEWER INDEPENDENCE	ADM

PURPOSE AND SUMMARY OF RESULTS:

Revision 1: This revision is a non-proprietary version of Revision 0.

The purpose of the present analysis is to determine from a fracture mechanics viewpoint the suitability of leaving degraded J-groove weld and butter material in the ANO Unit 1 reactor vessel head following the repair of a CRDM nozzle by the ID temper bead weld procedure. It is postulated that a small flaw in the head would combine with a large stress corrosion crack in the weld and butter to form a radial corner flaw that would propagate into the low alloy steel head by fatigue crack growth under cyclic loading conditions associated with heatup and cooldown.

Based on an evaluation of fatigue crack growth into the low alloy steel head, a postulated [ ]" radial crack in the Alloy 182 J-groove weld and butter would be acceptable from a fracture mechanics viewpoint for 25 years of operation.

THE FOLLOWING COMPUTER CODES HAVE BEEN USED IN THIS DOCUMENT:		THE DOCUMENT CONTAINS ASSUMPTIONS THAT MUST BE VERIFIED PRIOR TO USE ON SAFETY-RELATED WORK
CODE/VERSION/REV	CODE/VERSION/REV	☐ YES ☒ NO

RECORD OF REVISIONS

Revision	Affected Pages	Description of Revision	Date
0	All	Original release	11/02
1	All	Revision 1 is a non-proprietary version of Revision 0.	12/02

CONTENTS

Section	Heading	Page
1.0	Introduction	4
2.0	Geometry and Flaw Model	6
3.0	Material Properties	9
4.0	Fracture Mechanics Methodology	11
5.0	Applied Stresses	12
6.0	Flaw Evaluations	24
7.0	Summary of Results	36
8.0	References	37

Appendix	Heading	Page
A	Nozzle 56 Considerations	38
B	Certification Document	46
C	Letter from Entergy for Reactor Trip Transients	47

1.0 Introduction

Due to the susceptibility of Alloy 600 partial penetration nozzles to primary water stress corrosion cracking (PWSCC), an ID temper bead weld repair procedure has been developed for reactor vessel head control rod drive mechanism (CRDM) nozzles at ANO Unit 1 wherein the lower portion of a degraded nozzle is removed by a boring procedure and the remaining portion of the nozzle is welded to the low alloy steel reactor vessel head above the original Alloy 182 J-groove attachment weld, as shown in Figure 1. This repair design is more fully described by the design drawing [1] and the technical requirements document [2]. Except for a chamfer at the corner, the original J-groove weld will not be removed. Since a potential flaw in the J-groove weld can not be sized by currently available non-destructive examination techniques, it is assumed that the "as-left" condition of the remaining J-groove weld includes degraded or cracked weld material extending through the entire J-groove weld and Alloy 182 butter material. The purpose of the present analysis is to determine from a fracture mechanics viewpoint the suitability of leaving degraded J-groove weld material in the vessel following the repair of a CRDM nozzle by the ID temper bead weld procedure.

Since it is known from analysis of the ANO-1 CRDM reactor vessel head nozzle penetrations [3] that the hoop stress in the J-groove weld is greater than the axial stress at the same location, the preferential direction for cracking would be axial, or radial relative to the nozzle. It is postulated that a radial crack in the Alloy 182 weld metal would propagate by PWSCC, through the weld and butter, to the interface with the low alloy steel head. It is fully expected that such a crack would then blunt and arrest at the butter-to-head interface [4]. On the uphill side of the nozzle, where the hoop stresses are highest [3] and the area of the J-groove weld is the largest [1], a radial crack depth extending from the corner of the weld to the low alloy steel head would be very deep, about $1^3/_4$" for the outermost row of nozzles (closest to the head-to-vessel flange). Since the penetration angle decreases toward the center of the head, crack depths would be progressively less at each row of nozzles inward from the outermost row. For the present analysis of the remaining J-groove weld, it is postulated that a small fatigue initiated flaw forms in the low alloy steel head and combines with the stress corrosion crack in the weld to form a large radial corner flaw that would propagate into the low alloy steel head by fatigue crack growth under cyclic loading conditions associated with the normal condition heatup and cooldown transients and the upset condition reactor trip transient. The rod withdrawal accident transient, which is classified as an emergency condition transient for the repaired CRDM nozzle in Appendix B, is the most severe emergency or faulted condition transient for the J-groove weld region. The final flaw size is then evaluated for this rod withdrawal accident transient.

The size of the postulated flaw is to the depth of the J-groove weld prep as measured along the inside surface of the head penetration. The repair design [1] specifies that the inside corner of the J-groove weld is to be progressively chamfered from the center to outermost penetrations to maintain a constant [ ]" effective J-groove weld prep at all locations. Thus for the present analysis, [ ]" is used for the initial size of the postulated nozzle corner flaw in the low alloy steel head.

Nozzle 56 was previously repaired in April 2001 by partially removing an axial flaw in the J-groove weld and nozzle wall and welding with Alloy [ ] filler material. Appendix A presents an assessment of the effects of this repair on the flaw evaluation of the chamfered J-groove weld.

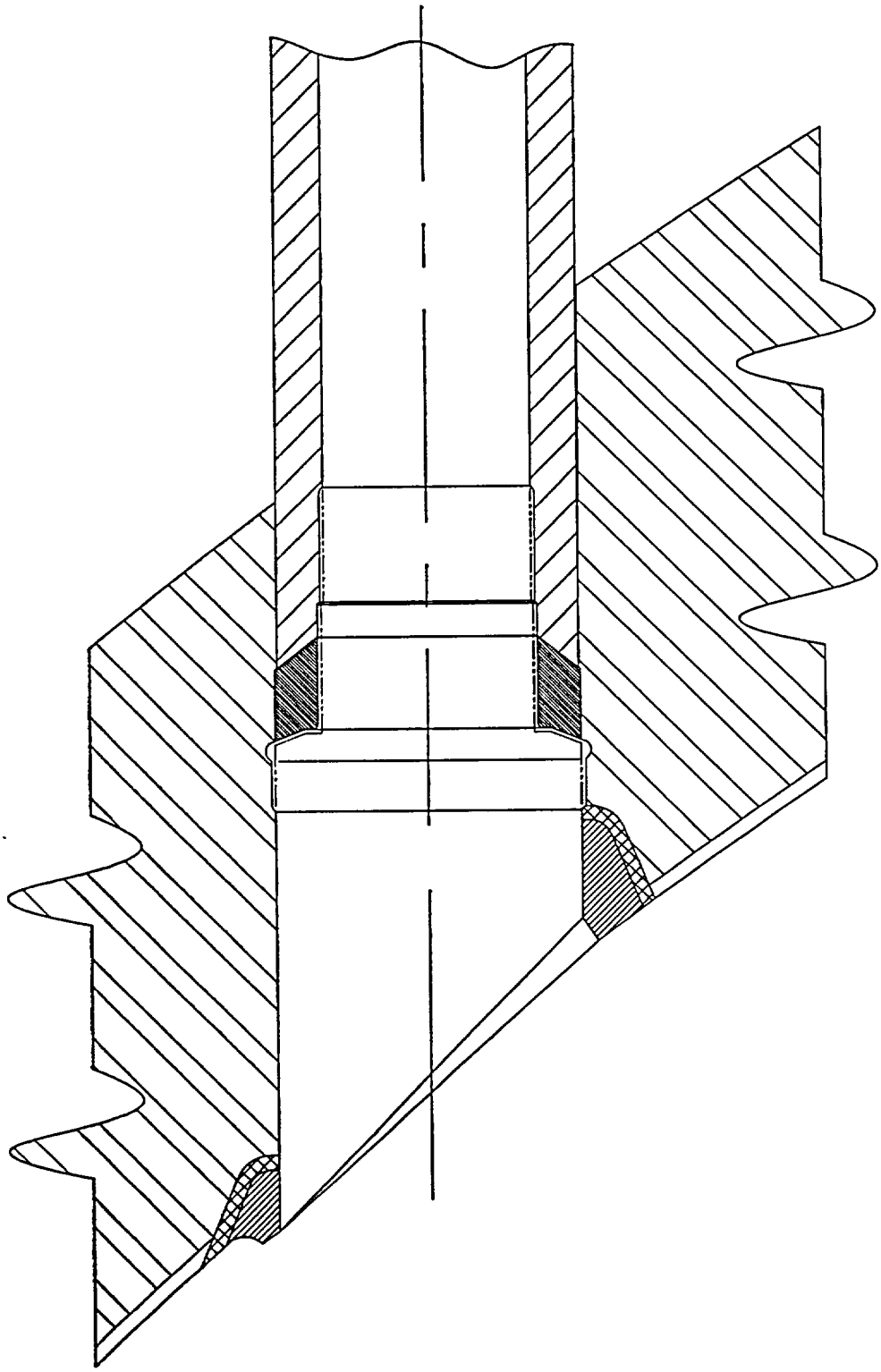

Figure 1. ID Temper Bead Weld Repair

2.0 Geometry and Flaw Model

It is postulated that a radial flaw is present in the low alloy steel head, extending from the chamfered corner of the remaining J-groove weld to the interface between the butter and head. Analytically, this flaw is crudely simulated using the corner flaw model shown below in Figure 2.

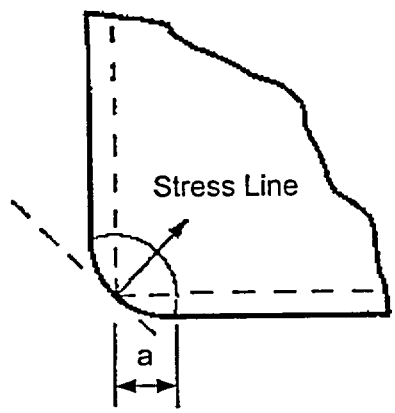

Figure 2. Corner Flaw Model

The flaw depth, "a", is the radius to the crack front. The stress line shown in the figure above depicts a typical direction for consideration of a one-dimensional variation of stress through the area represented by the corner flaw model.

The height of the original J-groove weld prep varies around the bore for all nozzle penetrations other than the one at the center of the head. In order to maintain a constant depth of remaining weld (and therefore postulated flaw depth) at all penetrations repaired by the ID temper bead repair procedure, the design drawing [1] specifies a chamfer at the inside corner of the J-groove weld to limit the height of the weld along the bored surface, from the inside corner to the low alloy steel head, to [ ]". Thus for the present flaw evaluations, the maximum initial flaw depth that need be considered is

a = [ ] in. [1].

Fatigue stresses for the ID temper bead repair are obtained from a three-dimensional finite element structural analysis [6] that determined operating stresses in the remaining CRDM nozzle, the new weld, the remaining J-groove weld, and the reactor vessel head. The finite element model of the extreme hillside nozzle (38.5° penetration angle) includes a detailed geometrical representation of the remaining J-groove weld prep around the penetration. Stresses are reported along a line originating at the inside corner (Point 0) and passing through the curved portion of the weld prep, as shown in Figure 3. The orientation of the stress line, relative to the vertical bored surface, is set at the maximum angle from the vertical (~15°) where the distance along the line, from Point 0 to the interface between the butter and head, is still nearly equal to the height of the weld along the bore.

The design drawing [1] specifies a [ ]" tolerance on the size of the chamfer (for example, [ ]" to [ ]" for nozzles 62 through 69), which could create a smaller remaining weld height than the [ ]" maximum. Although this would result in a smaller initial depth for the postulated flaw, the larger chamfer produces higher stresses in the weld. Accordingly, a maximum chamfer of [ ]" was included in the finite element model to provide an upper bound on stress (weld height is approximately [ ]"). This results in a conservative analytical strategy, wherein bounding stresses (based on a maximum chamfer of [ ]") are coupled with a maximum flaw depth (based on a minimum chamfer of [ ]") in the fracture mechanics analysis.

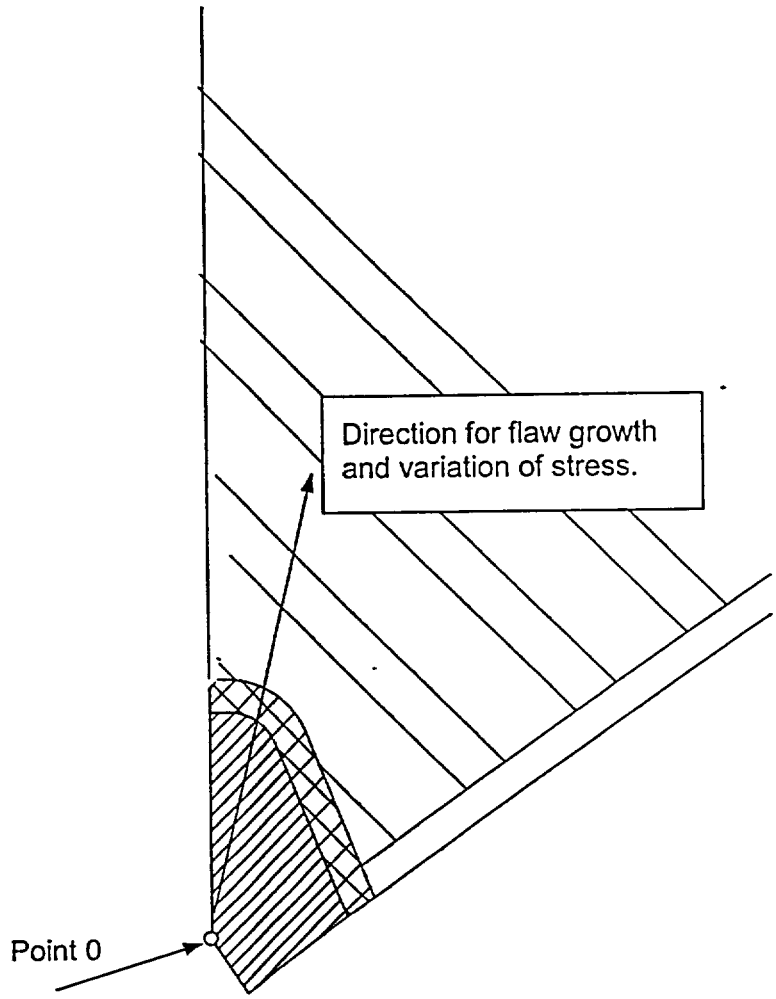

Figure 3. Orientation of Stress Line

3.0 Material Properties

The center portion of the ANO-1 reactor vessel head (closure head center disc) containing the CRDM nozzles is made from low alloy steel plate that is equivalent to [ ] material [5, 7].

Yield Strength

From the ASME Code, Section III, Appendix I [8], the minimum yield strength for the head material is 43.8 ksi at 600 °F. This is used as a conservative lower bound for yield strengths at operating temperatures less than 600 °F.

Reference Nil-Ductility Temperature

Based on a highest measured RT_{NDT} of [ ] °F for 13 heats of [ ] plate material [9], a value of [ ] °F is conservatively used as the RT_{NDT} of the [ ] low alloy steel head material.

Fracture Toughness

The lower bound K_{Ia} curve of Section XI, Appendix A, Figure A-4200-1 [10], which can be expressed as

$$K_{Ia} = 26.8 + 1.233 \exp [\, 0.0145 (T - RT_{NDT} + 160) \,] , \qquad [11]$$

represents the fracture toughness for crack arrest, where T is the crack tip temperature and RT_{NDT} is the reference nil-ductility temperature of the material. The corresponding fracture toughness curve for crack initiation is

$$K_{Ic} = 33.2 + 2.806 \exp [\, 0.02 (T - RT_{NDT} + 100) \,] . \qquad [11]$$

K_{Ia} and K_{Ic} are in terms of ksi√in and T and RT_{NDT} are in °F. In the present flaw evaluations, both measures of fracture toughness are limited to a maximum value of 200 ksi√in for upper-shelf fracture toughness. For an RT_{NDT} of [ ] °F, K_{Ia} and K_{Ic} equal 200 ksi√in at crack tip temperatures of 242 °F and 164 °F, respectively. The lowest service temperatures considered in the present flaw evaluations are 250 °F for normal and upset conditions and 600 °F for the emergency rod withdrawal accident transient, confirming that operation is in the upper-shelf region of the fracture toughness curves.

Fatigue Crack Growth

Flaw growth due to cyclic loading is calculated using the fatigue crack growth rate model from Article A-4300 of Section XI [10],

$$\frac{da}{dN} = C_o(\Delta K_I)^n,$$

where ΔK_I is the stress intensity factor range in ksi√in and da/dN is in inches/cycle. The crack growth rates for a surface flaw will be used for the evaluation of the corner crack since it is assumed that the degraded condition of the J-groove weld and butter exposes the low alloy steel head material to the primary water environment.

Fatigue Crack Growth Rates for Low Alloy Ferritic Steels in a Primary Water Environment

Source: ASME Code, Section XI, 1992 Edition with No Addenda [10]

$$\Delta KI = KI_{max} - KI_{min}$$
$$R = KI_{min} / KI_{max}$$

$0 \le R \le 0.25$: $\Delta K_I < 17.74$,

$n = 5.95$
$C_o = 1.02 \times 10^{-12} \times S$
$S = 1.0$

$\Delta K_I \ge 17.74$,

$n = 1.95$
$C_o = 1.01 \times 10^{-7} \times S$
$S = 1.0$

$0.25 \le R \le 0.65$: $\Delta K_I < 17.74\,[\,(3.75R + 0.06) / (26.9R - 5.725)\,]^{0.25}$,

$n = 5.95$
$C_o = 1.02 \times 10^{-12} \times S$
$S = 26.9R - 5.725$

$\Delta K_I \ge 17.74\,[\,(3.75R + 0.06) / (26.9R - 5.725)\,]^{0.25}$,

$n = 1.95$
$C_o = 1.01 \times 10^{-7} \times S$
$S = 3.75R + 0.06$

$0.65 \le R < 1.0$: $\Delta K_I < 12.04$,

$n = 5.95$
$C_o = 1.02 \times 10^{-12} \times S$
$S = 11.76$

$\Delta K_I \ge 12.04$,

$n = 1.95$
$C_o = 1.01 \times 10^{-7} \times S$
$S = 2.5$

4.0 Fracture Mechanics Methodology

The corner crack is analyzed using the following stress intensity factor solution:

$$K_I = \sqrt{\pi a}\left[0.706(A_0 + A_p) + 0.537\left(\frac{2a}{\pi}\right)A_1 + 0.448\left(\frac{a^2}{2}\right)A_2 + 0.393\left(\frac{4a^3}{3\pi}\right)A_3\right],$$

[Ref. 11, Eqn. (G-2.2)]

where a is the depth of the crack and A_p is a term added to the Reference 11 solution to account for pressure on the crack face.

The stress distribution in the radial direction is described by the third-order polynomial,

$$\sigma = A_0 + A_1 x + A_2 x^2 + A_3 x^3,$$ [Ref. 11, Eqn. (G-2.1)]

where x is measured from the inside corner of the chamfered weld, as shown in Figure 3.

From previous experience it is known that the corner crack model produces conservative results when compared to more rigorous stress intensity factor solutions calculated by the KCALC routine in the finite element code ANSYS.

Irwin Plasticity Correction

The Irwin plasticity correction is used to account for a moderate amount of yielding at the crack tip. For plane strain conditions, this correction is defined by

$$r_y = \frac{1}{6\pi}\left(\frac{K_I(a)}{\sigma_y}\right)^2,$$

where,

$K_I(a)$ = stress intensity factor based on the actual crack length, a,

σ_y = material yield strength.

A stress intensity factor, $K_I(a_e)$, is then calculated based on the effective crack length,

$$a_e = a + r_y.$$

5.0 Applied Stresses

Operational stresses are obtained from the results of a three-dimensional linear finite element analysis of the outermost CRDM nozzle head penetration that addresses the configuration after repair by the ID temper bead weld procedure of Reference 1. Stresses are available from Reference 6 at the 0°, 45°, 90°, 135°, and the 180° locations around the nozzle bore for various times during a combined normal and upset condition transient that includes heatup, cooldown, and a reactor trip. Additional stresses are available for the rod withdrawal accident transient, which is classified as an upset condition in the reactor coolant system functional specification [12]. Since ANO-1 has not experienced any of these transients during its plant life [14], the rod withdrawal accident is analyzed as an emergency condition transient, with no contribution to fatigue crack growth. This exception to the functional specification is noted in the document certification statement contained in Appendix B.

The 0° and 180° locations are at the downhill and uphill sides of the nozzle, respectively. Stresses were reported in a cylindrical coordinate system relative to the nozzle so that the stress directions remain constant around the nozzle. The largest hoop stresses are found at the uphill side of the nozzle bore, or at the 180° location. These stresses are perpendicular to the crack face and tend to open the corner crack. The operational stresses from Reference 6, calculated for the extreme outermost CRDM nozzle location, conservatively bound the stresses at all other nozzle locations.

The highest hoop stresses for the combined heatup-reactor trip-cooldown transient occur at 10.125 hours into the transient, during the reactor trip portion. Stresses are also significant at 4.8714 hours (heatup), 10.0 hours (steady state), and 12.939 hours (when the decay heat system is initiated during cooldown following a reactor trip). Due to the dominating influence of pressure on stress, stresses remain positive throughout the combined heatup-reactor trip-cooldown transient. The hoop stresses for these four loading conditions are listed in Table 1 for the uphill (180°) location as a function of the radial position along the stress line shown in Figures 2 and 3. The maximum stresses that occur during the rod withdrawal accident transient are listed in Table 2. Although stresses are reported for 13 positions along the stress line, ranging from 0" to 8.82" from the inside corner of the nozzle bore, only the first 7 positions are used to form a third-order polynomial stress fit over a distance of approximately 1.92" from the surface, which includes the weld area and a small portion of the reactor vessel head.

The functional specification for the reactor coolant system [12] specifies one emergency condition transient, a stuck open turbine bypass valve, and two faulted condition transients, a steam line break and a loss of coolant accident. The pressures and temperatures associated with these transients are evaluated in Appendix F of the stress analysis [6] against the governing upset reactor trip transient at 10.125 hours. Reference 6 concludes that the stresses resulting from these three transients are bounded by those for the analyzed reactor trip transient.

Table 1. Normal/Upset Condition Hoop Stresses [6]

Position Along Stress Line	Loading Condition			
	Heatup (HU)	Steady State (SS)	Reactor Trip (RT)	Cooldown (CD)
	Time = 4.8714 hr.	Time = 10.000 hr.	Time = 10.125 hr.	Time = 12.939 hr.
	Temp. = 559 °F	Temp. = 604 °F	Temp. = 531 °F	Temp. = 250 °F
	Pres. = [ ] psig	Pres. = [ ] psig	Pres. = [ ] psig	Pres. = [ ] psig
x (in.)	Stress (psi)	Stress (psi)	Stress (psi)	Stress (psi)
0.0000	[ ]	[ ]	[ ]	[ ]
0.2799	[ ]	[ ]	[ ]	[ ]
0.5597	[ ]	[ ]	[ ]	[ ]
0.8396	[ ]	[ ]	[ ]	[ ]
1.1195	[ ]	[ ]	[ ]	[ ]
1.5217	[ ]	[ ]	[ ]	[ ]
1.9238	[ ]	[ ]	[ ]	[ ]
2.3260	[ ]	[ ]	[ ]	[ ]
2.7282	[ ]	[ ]	[ ]	[ ]
4.2523	[ ]	[ ]	[ ]	[ ]
5.7764	[ ]	[ ]	[ ]	[ ]
7.3004	[ ]	[ ]	[ ]	[ ]
8.8245	[ ]	[ ]	[ ]	[ ]

Table 2. Emergency Condition Hoop Stresses [6]

Position Along Stress Line	Loading Condition
	Rod Withdrawal Accident (RWA)
	Time = 0.0044 hours
	Temperature = 600 °F
	Pressure = [ ] psig
x (in.)	Stress (psi)
0.0000	[ ]
0.2799	[ ]
0.5597	[ ]
0.8396	[ ]
1.1195	[ ]
1.5217	[ ]
1.9238	[ ]
2.3260	[ ]
2.7282	[ ]
4.2523	[ ]
5.7764	[ ]
7.3004	[ ]
8.8245	[ ]

Consideration of residual stresses

Two three-dimensional elastic-plastic finite element analyses [3] were performed by Dominion Engineering, Inc. (DEI) to simulate the sequence of steps involved in arriving at the configuration of the CRDM nozzle and reactor vessel head after completion of the ID temper bead repair. The first set of analyses used the finite element model depicted in Figure 4 to determine stresses for five combinations of nozzle angle and yield strength, as listed below.

DEI Analysis Cases

	Nozzle Angle*	Yield Strength
Center nozzle	0.0°	[ ] ksi
	18.2°	[ ] ksi
	26.2°	[ ] ksi
Outermost nozzle	38.5°	[ ] ksi
Outermost nozzle	38.5°	[ ] ksi

* Relative to center of head.

This analysis simulated the laying of the original weld butter and the subsequent post-weld stress relief, the heatup of the original J-groove weld and adjacent material during the welding process and the subsequent cooldown to ambient temperature, a pre-service hydro test, and operation at steady state conditions. After the steady state loads were removed and the structure was again at ambient conditions, the nozzle was removed from the model. The stresses associated with this repair configuration represent the residual stresses in the vicinity of the original J-groove weld, butter, and adjacent head, prior to chamfering the J-groove weld and completing the ID temper bead repair in the region above the J-groove weld. The residual stresses for the outermost penetration (38.5°) are listed in Table 3 and plotted in Figure 5.

The second analysis performed by Dominion Engineering addressed the final steps involved in completing the ID temper bead repair weld. For the sake of simplicity, the center nozzle was modeled in an axisymmetric analysis (Figure 6) to simulate the removal of the nozzle below the cut line [1], the deposition of the repair weld using four weld passes, and the chamfering of the J-groove weld (Figure 7). Although this analysis was performed for the center nozzle, the location of the repair weld above the J-groove and the size of the chamfer ([ ]") were specified to represent the worst case geometry at the outermost nozzle, where the distance between the two welds is a minimum and the size of the chamfer is a maximum. From the DEI analysis [3], the minimum vertical distance between welds is [ ]" (difference between the Z-coordinates of nodes 2009 and 1409). The final residual stresses for the representative penetration are listed in Table 4 and plotted in Figure 8.

Although at shutdown, the residual hoop stress in the weld region is high, above [ ] psi (Figures 5 and 8), the stress decreases to zero just beyond the butter region and is compressive in the head. These residual stresses would be relieved as the crack propagates through the

weld and butter and a short distance into the head. Deeper cracks would then experience only compressive residual stress ahead of the crack tip. It can be seen from Figure 8 and Table 4 that the residual stresses are compressive at some distance less than [ ]" into the head. The depth of the initial flaw size will therefore be increased by this amount so that residual stresses need not be considered in the present flaw evaluation.

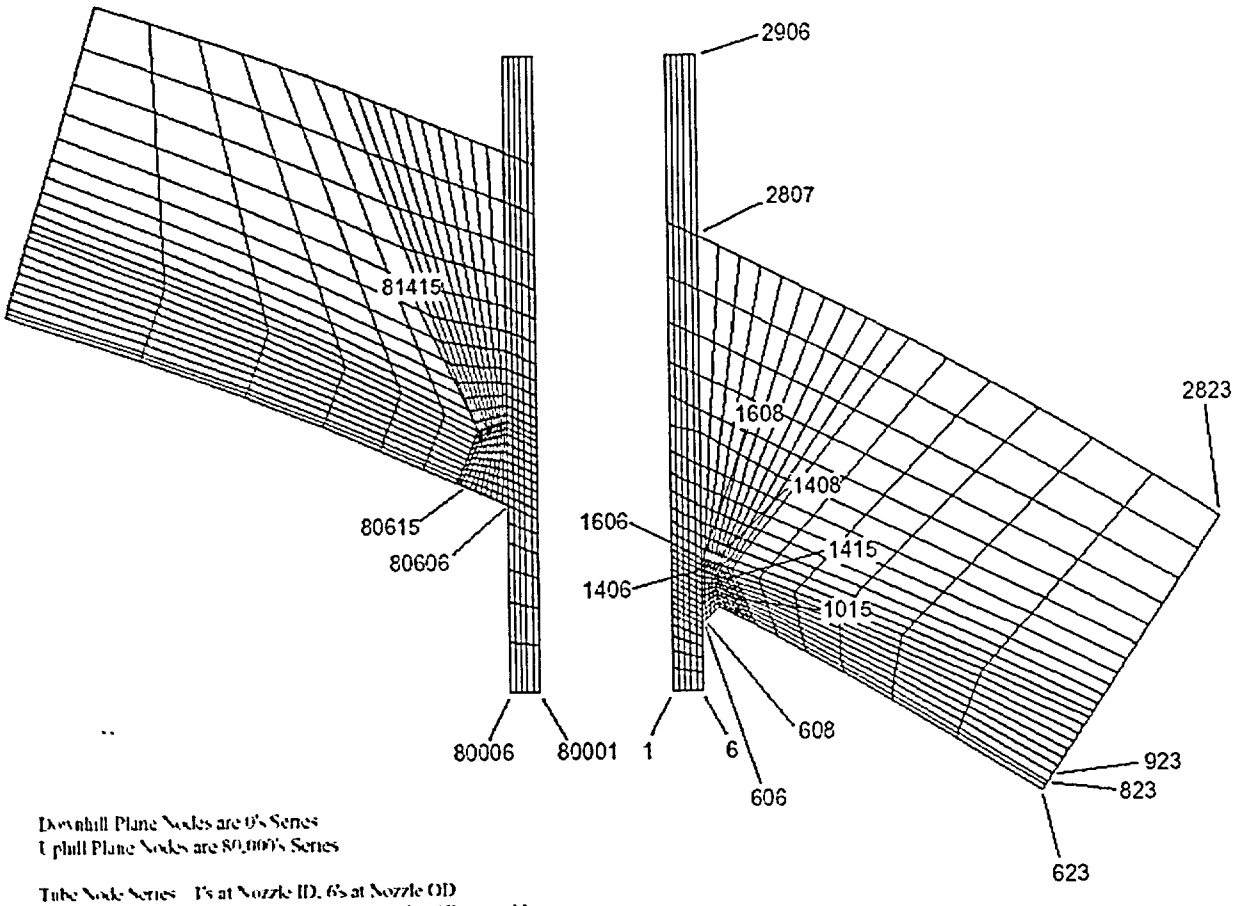

Downhill Plane Nodes are 0's Series
Uphill Plane Nodes are 80,000's Series

Tube Node Series 1's at Nozzle ID, 6's at Nozzle OD
Shell Node Series 6's at Shell ID (merged w. tube OD) in weld region
7's at Shell ID above weld region
23's at edge of shell section

Node Numbers Increase by 100 up the length of the tube and shell
Node Numbers Increase by 1 along the tube and shell radius

Figure 4. DEI Model for CRDM Nozzle Stress Analysis

Table 3.
Residual Hoop Stresses After Nozzle Removal

Penetration angle = 38.5 degrees
Nozzle yield strength = [ ] ksi

File: ANO1-38B.results.txt [3]
Time: 7006

Node	Global Coordinates X (in.)	Global Coordinates Z (in.)	ΔS[1] (in.)	Location	Hoop Stress (psi)	Distance into Head (in.)
80606	2.0000	69.680	0.000	Inside Surface of Weld	[	
80708	2.1128	69.976	0.317	Weld		
80808	2.1059	70.183	0.514	Weld		
80909	2.1979	70.440	0.785	Weld		
81010	2.2760	70.670	1.028	Weld		
81111	2.3403	70.874	1.242	Weld		
81212	2.3881	71.050	1.424	Weld		
81313	2.4246	71.202	1.580	Weld		
81415	2.5142	71.313	1.712	Weld/Butter Interface		
81516	2.5672	71.416	1.826	Butter		
81617	2.6230	71.511	1.934	Butter/Head Interface		0.000
81717	2.6869	71.726	2.158	Head		0.224
81817	2.7637	71.984	2.427	Head		0.493
81917	2.8558	72.295	2.751	Head		0.817
82017	2.9664	72.667	3.139	Head		1.205
82117	3.0992	73.114	3.606	Head		1.672
82217	3.2586	73.650	4.165	Head		2.231
82317	3.4499	74.294	4.836	Head		2.902
82417	3.6795	75.066	5.642	Head		3.708
82517	3.9551	75.994	6.610	Head		4.676
82617	4.2860	77.108	7.772	Head		5.838
82717	4.6832	78.444	9.166	Head		7.231
82817	5.1600	80.049	10.840	Head	]	8.906

[1] Distance from inside corner (node 80606) - see Figure 4.

Figure 5. Residual Hoop Stresses After Nozzle Removal for Outermost Penetration at 38.5°

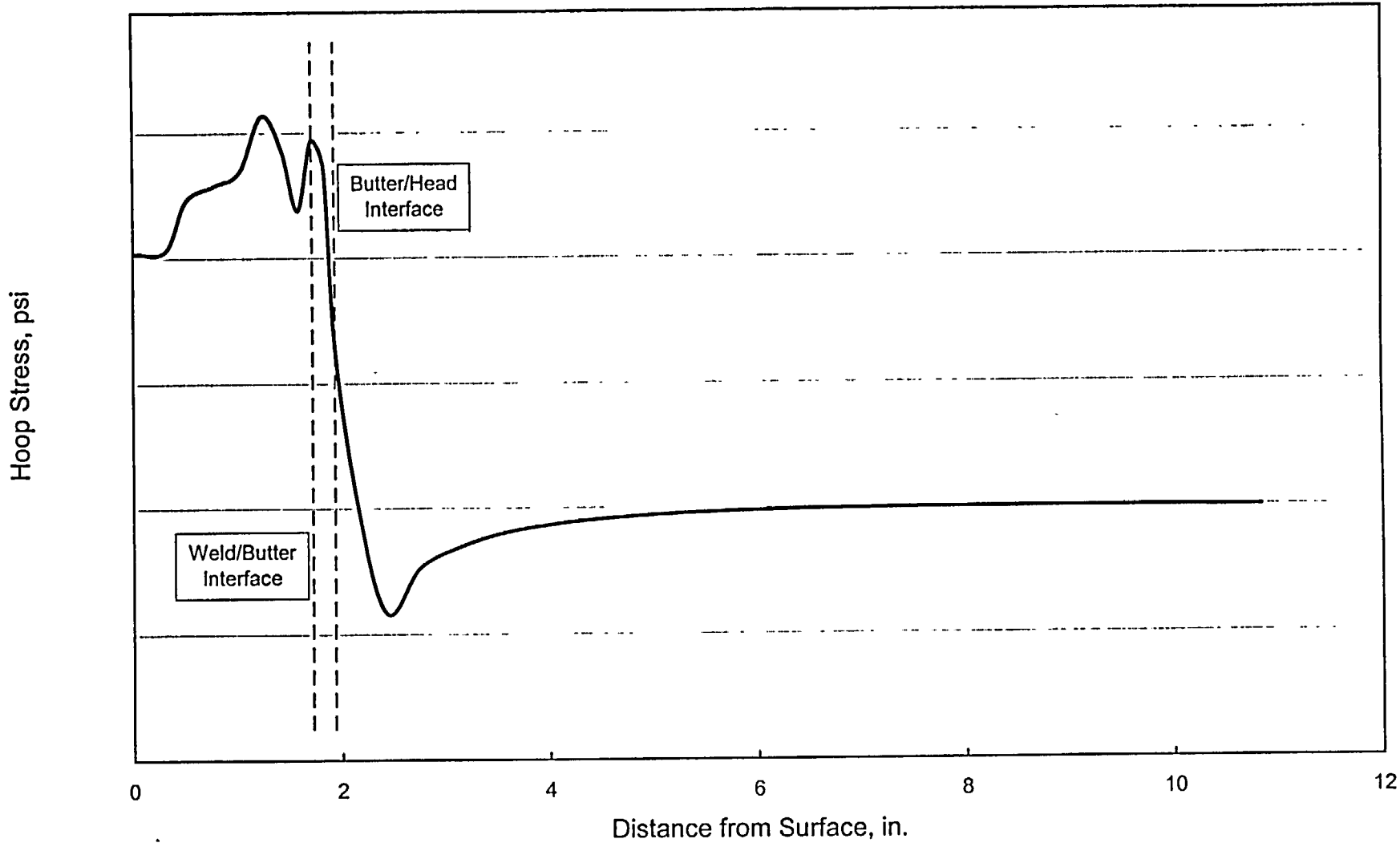

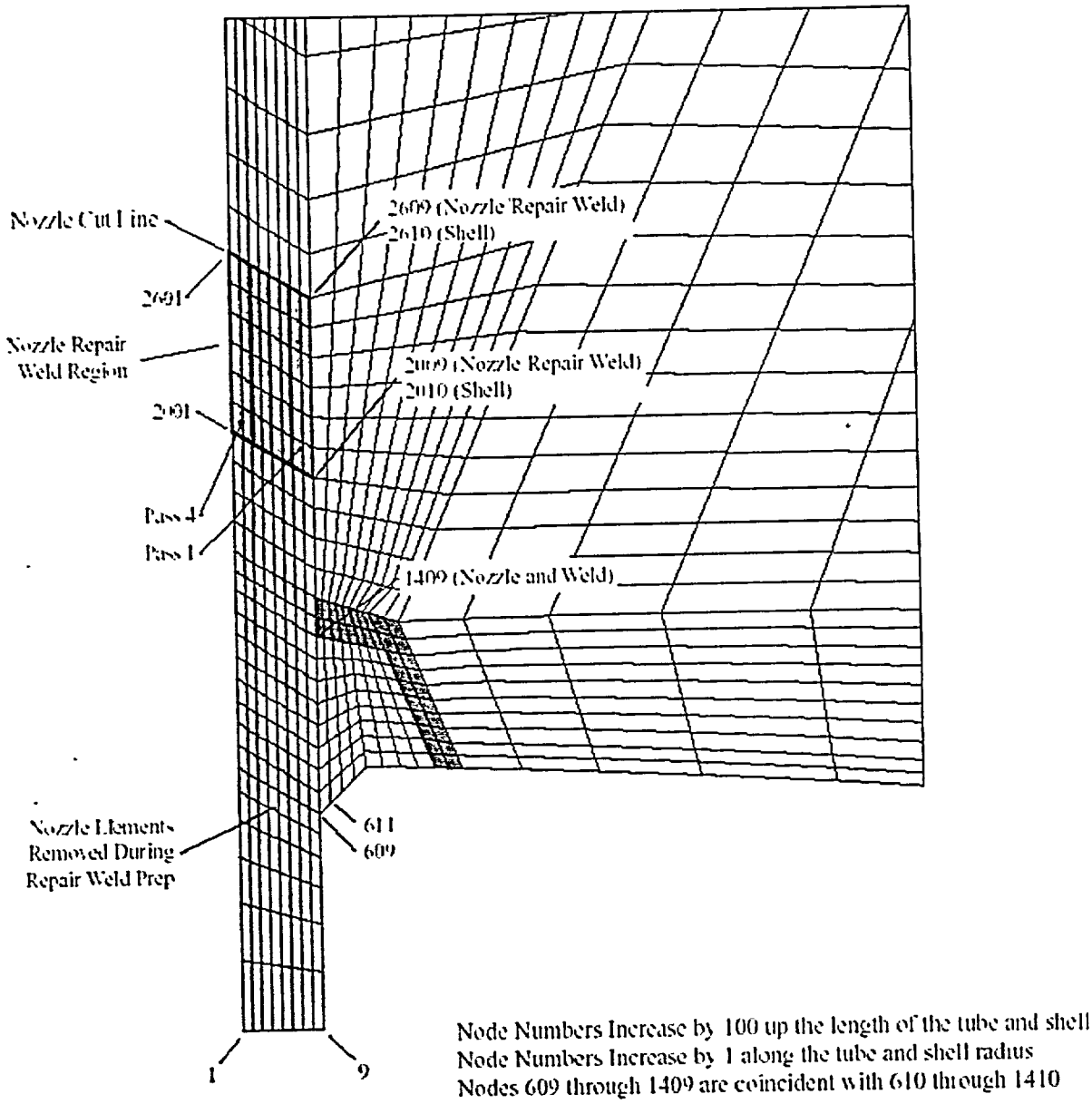

Figure 6. DEI Model for Center CRDM Nozzle with Weld Repair

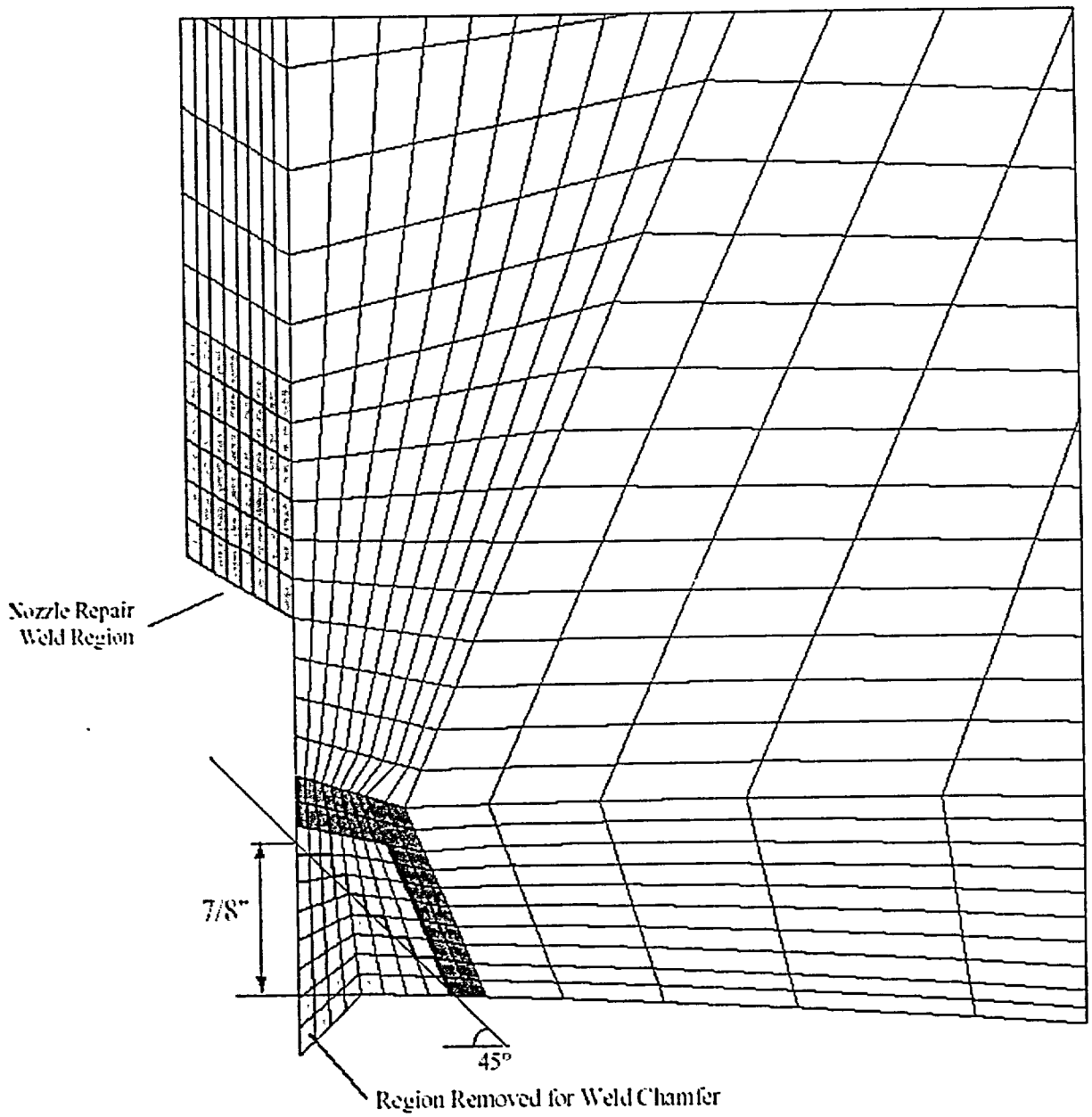

Figure 7. DEI Model for Center CRDM Nozzle After Weld Repair and Chamfer

Table 4.
Residual Hoop Stresses After Repair Weld and Chamfer

Penetration angle = 0 degrees
Nozzle yield strength = [ ] ksi

File: ANO1-0B.results.txt [3]
Time: 16001

Node	Global Coordinates X (in.)	Global Coordinates Z (in.)	ΔS[1] (in.)	Location	Hoop Stress (psi)	Distance into Head (in.)
	2.0000	86.686	0.000	Inside Surface of Weld		
	2.0852	86.924	0.253	Weld		
	2.0821	87.077	0.400	Weld		
	2.1579	87.278	0.613	Weld		
	2.2273	87.453	0.800	Weld		
1114	2.2905	87.604	0.963	Weld	[ ]	
1215	2.3572	87.708	1.083	Weld		
1316	2.4077	87.809	1.195	Weld		
1418	2.5053	87.893	1.309	Weld/Butter Interface		
1519	2.5578	88.002	1.429	Butter		
1620	2.6141	88.100	1.542	Butter/Head Interface		0.000
1720	2.6933	88.286	1.744	Head		0.202
1820	2.7850	88.501	1.977	Head		0.436
1920	2.8911	88.749	2.247	Head		0.706
2020	3.0140	89.037	2.560	Head		1.019
2120	3.1562	89.370	2.922	Head		1.381
2220	3.3209	89.756	3.342	Head		1.801
2320	3.5114	90.203	3.828	Head		2.286
2420	3.7320	90.720	4.390	Head		2.849
2520	3.9874	91.318	5.040	Head		3.499
2620	4.2830	92.011	5.794	Head		4.252
2720	4.6251	92.813	6.666	Head		5.124
2820	5.0212	93.741	7.675	Head		6.133

[1] Distance from original inside corner (node 609) - see Figure 6.

Figure 8. Residual Hoop Stresses After Repair Weld and Chamfer for Representative Penetration

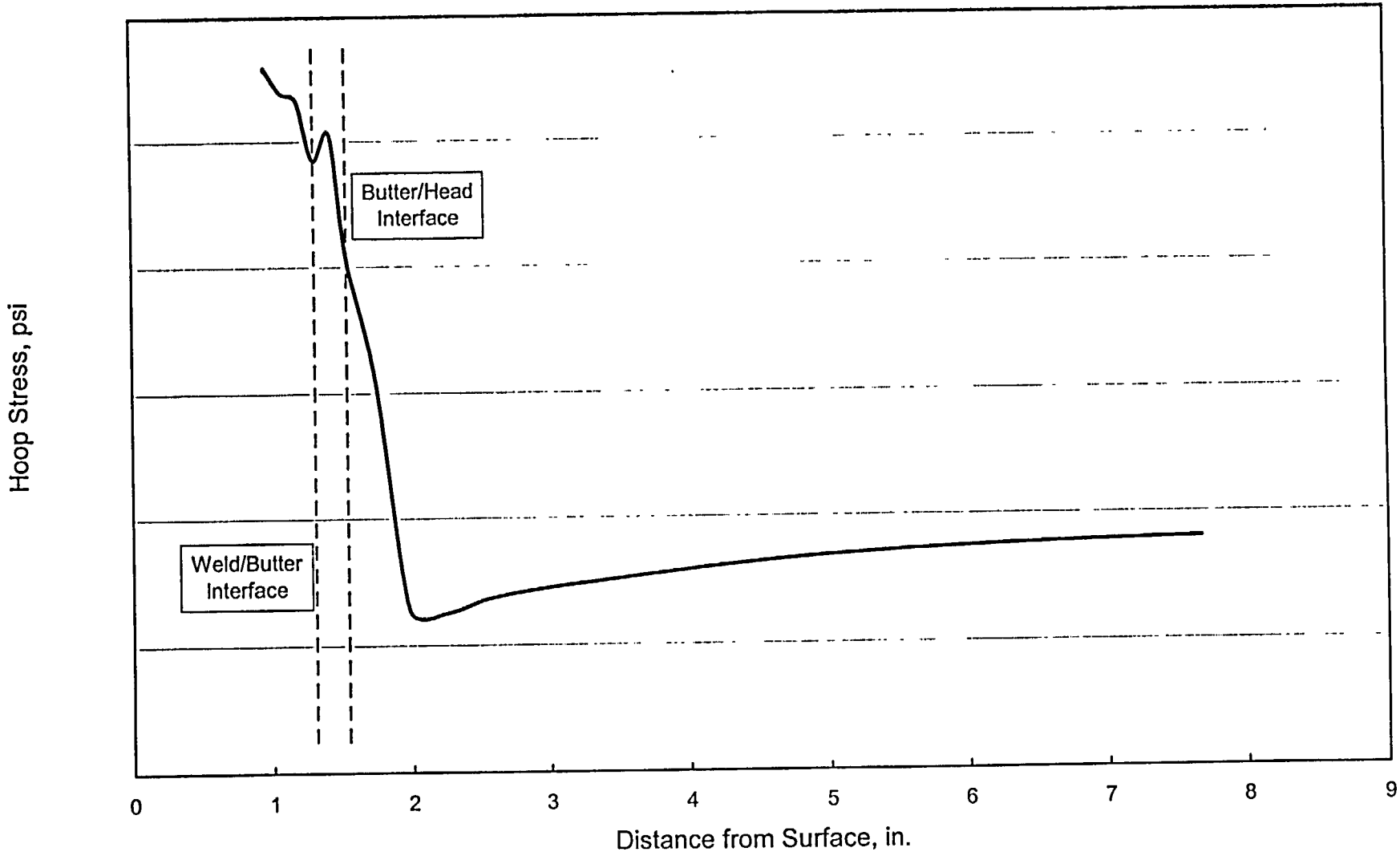

6.0 Flaw Evaluations

The actual fracture mechanics calculations are presented in Tables 5 through 7. Evaluations are performed for a postulated radial corner crack on the uphill side of the outermost CRDM nozzle head penetration. The applicable hoop stresses (perpendicular to the plane of the postulated crack) are listed in Tables 1 and 2 for key time points from the finite element stress analysis [6].

As required by Article IWB-3612 [10], a safety factor of $\sqrt{10}$ is used for normal and upset conditions with the lower K_{Ia} fracture toughness for crack arrest. Article IWB-3612 also specifies that a safety factor of $\sqrt{2}$ must be used for emergency and faulted conditions, along with the higher K_{Ic} fracture toughness for crack initiation. As discussed in Section 5.0, the reactor trip stresses bound the emergency and faulted condition stresses. The flaw evaluation performed for the reactor trip transient therefore serves as a bounding analysis for the emergency and faulted condition analysis required by IWB-3612 (excluding the rod withdrawal accident that is classified as an emergency condition for the present analysis).

Based on the stresses listed in Tables 1 and 2, two groups of transient conditions are considered for fatigue crack growth. For the heatup/cooldown transient, the bounding load pair consists of heatup at 4.8714 hours and shutdown (zero stress state). Reactor trip stresses at 10.125 hours and steady state stresses at 10.0 hours are used for the reactor trip cyclic load conditions.

Fatigue crack growth is calculated on a yearly basis using the following pattern for accumulating cycles:

Fatigue Crack Growth Cycles		
Transient	Heatup / Cooldown	Reactor Trip
Cycles / 40 Years	240	400
Cycles / Year	6	10

These cycles are distributed uniformly over the 25 year service life by linking the incremental crack growth between Table 5 (for heatup and cooldown) and Table 6 (for reactor trip). The final flaw size is evaluated in Table 7 for the rod withdrawal accident.

Table 5. Evaluation of CRDM Nozzle Corner Crack for Heatup/Cooldown

INPUT DATA

Initial Flaw Size: Distance to base metal: [ ] in.
Additional distance to compressive zone: [ ] in.

Total depth, a = [ ] in.

Material Data: Yield strength, S_y = 43.8 ksi

Reference temp., RTndt = [ ] F
Upper shelf tough. = 200 ksi√in

Kia = 26.8 + 1.233 exp [0.0145 (T - RTndt + 160)]

Kia is limited to the upper shelf toughness.

Applied Loads:

	Loading Conditions	
	HU*	SD**
	Temperature (F)	
	559	70
	Pressure, p (ksi)	
	Kia (ksi√in)	
Position	200	41
x	Hoop Stress	
(in.)	(ksi)	(ksi)
0.0000		
0.2799		
0.5597		
0.8396		
1.1195		
1.5217		
1.9238		
2.3260		
2.7282		
4.2523		
5.7764		
7.3004		
8.8245		

* Heatup at 4.8714 hours
** Shutdown

Table 5. Evaluation of CRDM Nozzle Corner Crack for Heatup/Cooldown (Cont'd)

STRESS INTENSITY FACTOR

$$KI(a) = \sqrt{(\pi a)}\,[\,0.706(A_0+A_p) + 0.537(2a/\pi)A_1 + 0.448(a^2/2)A_2 + 0.393(4a^3/3\pi)A_3\,]$$

where the through-wall stress distribution is described by the third order polynomial,

$$S(x) = A_0 + A_1x + A_2x^2 + A_3x^3,$$

defined by:

Stress Coeff.	Loading Conditions	
	HU	SD
	(ksi)	(ksi)
A_0		
A_1		
A_2		
A_3		

Effective crack size:

$$a_e = a + 1/(6\pi)^*[KI(a)/S_y]^2$$

Effective stress intensity factor:

$$KI(a_e) = \sqrt{(\pi a_e)}\,[\,0.706(A_0+A_p) + 0.537(2a_e/\pi)A_1 + 0.448(a_e^2/2)A_2 + 0.393(4a_e^3/3\pi)A_3\,]$$

Table 5. Evaluation of CRDM Nozzle Corner Crack for Heatup/Cooldown (Cont'd)

FATIGUE CRACK GROWTH

Transient Description: 240 cycles over 40 years

ΔN = 6 cycles/year

Operating Time (yr.)	Cycle	a (in.)	HU KI(a) (ksi√in)	SD KI(a) (ksi√in)	ΔKI (ksi√in)	Δa (in.)	HU a_e (in.)	SD a_e (in.)	HU KI(a_e) (ksi√in)	SD KI(a_e) (ksi√in)
0.0	0		46.29	0.00	46.29	0.00107			46.80	0.00
1.0	6		46.31	0.00	46.31	0.00107			46.81	0.00
2.0	12		46.32	0.00	46.32	0.00107			46.83	0.00
3.0	18		46.34	0.00	46.34	0.00107			46.84	0.00
4.0	24		46.35	0 00	46.35	0.00107			46.86	0.00
5.0	30		46.36	0.00	46.36	0.00108			46.87	0.00
6.0	36		46.38	0.00	46.38	0.00108			46.88	0.00
7.0	42		46.39	0.00	46.39	0.00108			46.90	0.00
8.0	48		46.41	0.00	46.41	0.00108			46.91	0.00
9.0	54		46.42	0.00	46.42	0.00108			46.93	0.00
10.0	60		46.44	0.00	46.44	0.00108			46.94	0.00
11.0	66		46.45	0.00	46.45	0.00108			46.95	0.00
12.0	72		46.46	0.00	46.46	0.00108			46.97	0.00
13.0	78		46.48	0.00	46.48	0.00108			46.98	0.00
14.0	84		46.49	0.00	46.49	0.00108			47.00	0 00
15.0	90		46.51	0.00	46.51	0.00108			47.01	0.00
16.0	96		46.52	0.00	46.52	0.00108			47.02	0.00
17.0	102		46.53	0.00	46.53	0.00108			47.04	0.00
18.0	108		46.55	0.00	46.55	0.00108			47.05	0.00
19.0	114		46.56	0.00	46.56	0.00108			47.07	0 00
20.0	120		46.58	0.00	46.58	0.00108			47.08	0.00
21.0	126		46.59	0.00	46.59	0.00109			47.09	0.00
22.0	132		46.61	0.00	46.61	0.00109			47.11	0.00
23.0	138		46.62	0.00	46.62	0.00109			47.12	0.00
24.0	144		46.63	0.00	46.63	0.00109			47.13	0.00
25.0	150		46.65	0.00	46.65	0.00109			47.15	0.00

Table 5. Evaluation of CRDM Nozzle Corner Crack for Heatup/Cooldown (Cont'd)

FRACTURE TOUGHNESS MARGINS

Period of Operation: Time = 25.0 years

Final Flaw Size: a = [ ] in. (after reactor trip)

Margin = KIa / KI(a_e)

	Loading Conditions		
	HU	SD	
Fracture Toughness, KIa	200.0	41.3	ksi√in
KI(a)	46.66	0.00	ksi√in
a_e			
KI(a_e)	47.16	0.00	ksi√in
Actual Margin	4.24	#N/A	
Required Margin	3.16	#N/A	

Table 6. Evaluation of CRDM Nozzle Corner Crack for Reactor Trip

INPUT DATA

Beginning Flaw Size: Depth, a = [ ] in.

Material Data: Yield strength, S_y = 43.8 ksi

Reference temp., RTndt = [ ] F
Upper shelf tough. = 200 ksi√in

Kla = 26.8 + 1.233 exp [0.0145 (T - RTndt + 160)]

Kla is limited to the upper shelf toughness.

Applied Loads:

	Loading Conditions	
	RT*	SS**
	Temperature (F)	
	531	604
	Pressure, p (ksi)	
	Kla (ksi√in)	
Position	200	200
x	Hoop Stress	
(in.)	(ksi)	(ksi)
0.0000		
0.2799		
0.5597		
0.8396		
1.1195		
1.5217		
1.9238		
2.3260		
2.7282		
4.2523		
5.7764		
7.3004		
8.8245		

* Reactor Trip at 10.125 hours
** Steady State at 10.000 hours

Table 6. Evaluation of CRDM Nozzle Corner Crack for Reactor Trip (Cont'd)

STRESS INTENSITY FACTOR

$$KI(a) = \sqrt{(\pi a)}\ [\ 0.706(A_0+A_p) + 0.537(2a/\pi)A_1 + 0.448(a^2/2)A_2 + 0.393(4a^3/3\pi)A_3\ ]$$

where the through-wall stress distribution is described by the third order polynomial,

$$S(x) = A_0 + A_1x + A_2x^2 + A_3x^3,$$

defined by:

Stress Coeff.	Loading Conditions	
	RT	SS
	(ksi)	(ksi)
A_0		
A_1		
A_2		
A_3		

Effective crack size:

$$a_e = a + 1/(6\pi)^*[KI(a)/S_y]^2$$

Effective stress intensity factor:

$$KI(a_e) = \sqrt{(\pi a_e)}\ [\ 0.706(A_0+A_p) + 0.537(2a_e/\pi)A_1 + 0.448(a_e^2/2)A_2 + 0.393(4a_e^3/3\pi)A_3\ ]$$

Table 6. Evaluation of CRDM Nozzle Corner Crack for Reactor Trip (Cont'd)

FATIGUE CRACK GROWTH

Transient Description: 400 cycles over 40 years

ΔN = 10 cycles/year

Operating Time (yr.)	Cycle	a (in.)	RT KI(a) (ksi√in)	SS KI(a) (ksi√in)	ΔKI (ksi√in)	Δa (in.)	RT a_e (in.)	SS a_e (in.)	RT KI(a_e) (ksi√in)	SS KI(a_e) (ksi√in)
0.0	0		60.92	44.80	16.12	0.00057			61.63	45.28
1.0	10		60.93	44.81	16.12	0.00057			61.64	45.29
2.0	20		60.94	44.83	16.11	0.00057			61.65	45.31
3.0	30		60.95	44.84	16.11	0.00057			61.66	45.32
4.0	40		60.96	44.86	16.11	0.00057			61.67	45.33
5.0	50		60.98	44.87	16.11	0.00057			61.69	45.35
6.0	60		60.99	44.88	16.10	0.00057			61.70	45.36
7.0	70		61.00	44.90	16.10	0.00057			61.71	45.38
8.0	80		61.01	44.91	16.10	0.00057			61.72	45.39
9.0	90		61.03	44.93	16.10	0.00057			61.73	45.40
10.0	100		61.04	44.94	16.10	0.00057			61.74	45.42
11.0	110		61.05	44.96	16.09	0.00057			61.75	45.43
12.0	120		61.06	44.97	16.09	0.00057			61.76	45.45
13.0	130		61.07	44.98	16.09	0.00057			61.77	45.46
14.0	140		61.09	45.00	16.09	0.00057			61.78	45.48
15.0	150		61.10	45.01	16.08	0.00057			61.79	45.49
16.0	160		61.11	45.03	16.08	0.00057			61.80	45.50
17.0	170		61.12	45.04	16.08	0.00057			61.81	45.52
18.0	180		61.13	45.06	16.08	0.00057			61.82	45.53
19.0	190		61.15	45.07	16.08	0.00057			61.83	45.55
20.0	200		61.16	45.08	16.07	0.00057			61.84	45.56
21.0	210		61.17	45.10	16.07	0.00057			61.85	45.57
22.0	220		61.18	45.11	16.07	0.00057			61.86	45.59
23.0	230		61.19	45.13	16.07	0.00057			61.87	45.60
24.0	240		61.20	45.14	16.06	0.00057			61.88	45.62
25.0	250		61.22	45.16	16.06	0.00057			61.89	45.63

Table 6. Evaluation of CRDM Nozzle Corner Crack for Reactor Trip (Cont'd)

FRACTURE TOUGHNESS MARGINS

Period of Operation: Time = 25.0 years

Final Flaw Size: a = [ ] in.

Margin = KIa / KI(a_e)

	Loading Conditions		
	RT	SS	
Fracture Toughness, KIa	200.0	200.0	ksi√in
KI(a)	61.22	45.16	ksi√in
a_e			
KI(a_e)	61.89	45.63	ksi√in
Actual Margin	3.23	4.38	
Required Margin	3.16	3.16	

Table 7. Evaluation of CRDM Nozzle Corner Crack for Rod Withdrawal Accident

INPUT DATA

Final Flaw Size: Depth, a = [ ] in. (after reactor trip)

Material Data: Yield strength, S_y = 43.8 ksi

Reference temp., RTndt = [ ] F
Upper shelf tough. = 200 ksi√in

Klc = 33.2 + 2.806 exp [0.02 (T - RTndt + 100)]

Klc is limited to the upper shelf toughness.

Applied Loads:

	Loading Conditions	
	RWA*	#N/A
	Temperature (F)	
	600	#N/A
	Pressure, p (ksi)	
		#N/A
	Klc (ksi√in)	
Position	200	#N/A
x	Hoop Stress	
(in.)	(ksi)	(ksi)
0.0000		#N/A
0.2799		#N/A
0.5597		#N/A
0.8396		#N/A
1.1195		#N/A
1.5217		#N/A
1.9238		#N/A
2.3260		#N/A
2.7282		#N/A
4.2523		#N/A
5.7764		#N/A
7.3004		#N/A
8.8245		#N/A

* Rod Withdrawal Accident at 0.0044 hours

Table 7. Evaluation of CRDM Nozzle Corner Crack for Rod Withdrawal Accident (Cont'd)

STRESS INTENSITY FACTOR

$$KI(a) = \sqrt{(\pi a)}\,[\,0.706(A_0+A_p) + 0.537(2a/\pi)A_1 + 0.448(a^2/2)A_2 + 0.393(4a^3/3\pi)A_3\,]$$

where the through-wall stress distribution is described by the third order polynomial,

$$S(x) = A_0 + A_1x + A_2x^2 + A_3x^3,$$

defined by:

Stress Coeff.	Loading Conditions	
	RWA	#N/A
	(ksi)	(ksi)
A_0		#N/A
A_1		#N/A
A_2		#N/A
A_3		#N/A

Effective crack size:

$$a_e = a + 1/(6\pi)*[KI(a)/S_y]^2$$

Effective stress intensity factor:

$$KI(a_e) = \sqrt{(\pi a_e)}\,[\,0.706(A_0+A_p) + 0.537(2a_e/\pi)A_1 + 0.448(a_e^2/2)A_2 + 0.393(4a_e^3/3\pi)A_3\,]$$

Table 7. Evaluation of CRDM Nozzle Corner Crack for Rod Withdrawal Accident (Cont'd)

FRACTURE TOUGHNESS MARGINS

Period of Operation: Time = 25.0 years

Final Flaw Size: a = [ ] in.

Margin = KIc / KI(a_e)

	Loading Conditions		
	RWA	#N/A	
Fracture Toughness, KIc	200.0	#N/A	ksi√in
KI(a)	66.99	#N/A	ksi√in
a_e		#N/A	
KI(a_e)	68.34	#N/A	ksi√in
Actual Margin	2.93	#N/A	
Required Margin	1.41	#N/A	

7.0 Summary of Results

A fracture mechanics analysis has been performed to evaluate a postulated large radial crack in the remnants of the original J-groove weld and butter after an ID temper bead repair of a CRDM nozzle reactor vessel head penetration. Results of this analysis are summarized below for the controlling transients.

Reactor Trip at 10.125 hours (Upset Condition)

Temperature,	$T = 531\ °F$
Initial flaw size,	$a_i = [\quad]$ in.
Final flaw size after 25 years,	$a_f = [\quad]$ in.
Flaw growth,	$a_f - a_i = 0.042$ in.
Stress intensity factor at final flaw size,	$K_I = 61.89$ ksi$\sqrt{in}$
Fracture toughness at 531 °F,	$K_{Ia} = 200.0$ ksi$\sqrt{in}$
Safety margin,	$K_{Ia} / K_I = 3.23 > \sqrt{10} = 3.16$

Rod Withdrawal Accident at 0.0044 hours (Emergency Condition)

Temperature,	$T = 600\ °F$
Flaw size at 25 years,	$a = [\quad]$ in.
Stress intensity factor,	$K_I = 68.34$ ksi$\sqrt{in}$
Fracture toughness at 531 °F,	$K_{Ia} = 200.0$ ksi$\sqrt{in}$
Safety margin,	$K_{Ia} / K_I = 2.93 > \sqrt{2} = 1.41$

Conclusion

Based on an evaluation of fatigue crack growth into the low alloy steel head, the above results demonstrate that a postulated radial crack in the Alloy 182 J-groove weld and butter would be acceptable for 25 years of operation.

8.0 References

1. Framatome ANP Drawing 02-5021508E-2, "CRDM Nozzle ID Temper Bead Weld Repair, ANO-1."

2. Framatome ANP Document 51-5021517-01, "ANO-1 CRDM Nozzle ID Ambient Temperature Temper Bead Weld Repair Requirements," November 2002.

3. Framatome ANP Document 38-1290261-00, ANO Design Input Record No. 2001-0230-020-02, dated 11/6/2002 forwarding Dominion Engineering Stress Calculations for IDTB Weld Repair.

4. Framatome ANP Document 51-5012047-00, "Stress Corrosion Cracking of Low Alloy Steel," March 2001.

5. Framatome ANP Drawing 02-135579E-9, "Closure Head Sub-Assembly," ANO-1.

6. Framatome ANP Document 32-5012424-10, "CRDM Temperbead Bore Weld Analysis," November 2002.

7. Framatome ANP Drawing 02-139669E-10, "Material List – Head and Vessel," ANO-1.

8. ASME Boiler and Pressure Vessel Code, Section III, Rules for Construction of Nuclear Power Plant Components, Division 1 - Appendices, 1989 Edition with No Addenda.

9. BAW-10046A, Rev. 2, "Methods of Compliance With Fracture Toughness and Operational Requirements of 10 CFR 50, Appendix G," B&W Owners Group Materials Committee Topical Report, June 1986.

10. ASME Boiler and Pressure Vessel Code, Section XI, Rules for Inservice Inspection of Nuclear Power Plant Components, 1992 Edition with No Addenda.

11. Marston, T.U., "Flaw Evaluation Procedures – Background and Application of ASME Section XI, Appendix A," EPRI Report NP-719-SR, August 1978.

12. Framatome ANP Document 18-1173987-03, "RCS Functional Specification for ANO-1."

13. Framatome ANP Document 38-1290260-00, ANO Design Input Record No. 2001-0230-020-01, dated 11/4/2002 forwarding Dominion Engineering Stress Results for Nozzle 56.

14. Letter from Entergy for Reactor Trip Transients, November 8, 2002 (attached as Appendix C).

Appendix A

Nozzle 56 Considerations

Nozzle 56 was previously repaired in April 2001 by partially removing an axial flaw in the J-groove weld and nozzle wall and welding with Alloy [ ] filler material. Dominion Engineering, Inc. (DEI) analyzed the final repair configuration and treated the remaining flaw indication as an embedded flaw. The flaw was modeled as a purely axial flaw in the nozzle (Figure A-1), starting at the nozzle outside surface at the top of the J-groove weld and extending 0.2" radially inward (toward the inside surface) and 1.3" axially upward (along the outside surface of the nozzle). In order to locate a plane of nodes at the center of the weld repair, the repair was modeled as extending over a total of 90 degrees, starting at the downhill position, with the flaw at the center of the 90 degree extent (or 45 degrees from the downhill position).

Dominion Engineering's embedded flaw model for Nozzle 56 is shown in Figure A-1 for a plane oriented 45° from the downhill position. Figure A-1 also indicates the node numbering scheme used for their finite element analysis. The nodes located in the same circumferential plane as the embedded flaw, or 45 degrees from the downhill position, are in the 20,000's range. In addition, for nodes on the open face of the crack (i.e., everywhere but the crack edges), the nodes are "doubled" to allow the crack face to open, and the doubled node numbers are increased by 300,000. On the crack face, the original 20,000's series nodes are kept on the elements closest to the downhill side of the model and the new 320,000's series nodes are transferred to the elements closer to the uphill side of the model.

The effect of the previous weld repair on Nozzle 56 will be assessed by comparing operating hoop stresses for both unrepaired and repaired nozzles. The angular penetration and yield strength of Nozzle 56 places this nozzle within the group modeled at 38.5° and 48.5 ksi yield. The model for an original CRDM nozzle is shown in Figure 4. Stresses are obtained along a path from the inside corner of the J-groove weld, through the weld and butter, and out into the head, as indicated in Tables A-1 and A-2 for the unrepaired and repaired nozzles, respectively. These stresses are plotted in Figures A-2 and A-3. In the DEI analyses, stresses at operation include residual stresses from welding and stresses due to pressure and temperature at steady state conditions.

Since the weld sizes are different for the two models, the distance along the stress paths differ for a common point of reference, say the weld-to-butter interface. Table A-3 provides a basis for comparing the results by listing stresses by their relative position along each path line. These "normalized" stresses are plotted in Figure A-4 for the unrepaired and repaired nozzles. Figure A-4 reveals that the operating stresses are higher for the unrepaired nozzle in the butter and head regions of the structure, where the influence of residual stress diminishes. The higher stress in the weld region for the repaired nozzle is due to an increase in residual stress from the deposition of the Alloy [ ] weld filler. These stresses would be relieved as a postulated PWSCC flaw in the J-groove weld propagated through the weld and butter. Thus the repairs made to Nozzle 56 do not adversely affect the results of the J-groove weld flaw evaluation contained in this document.

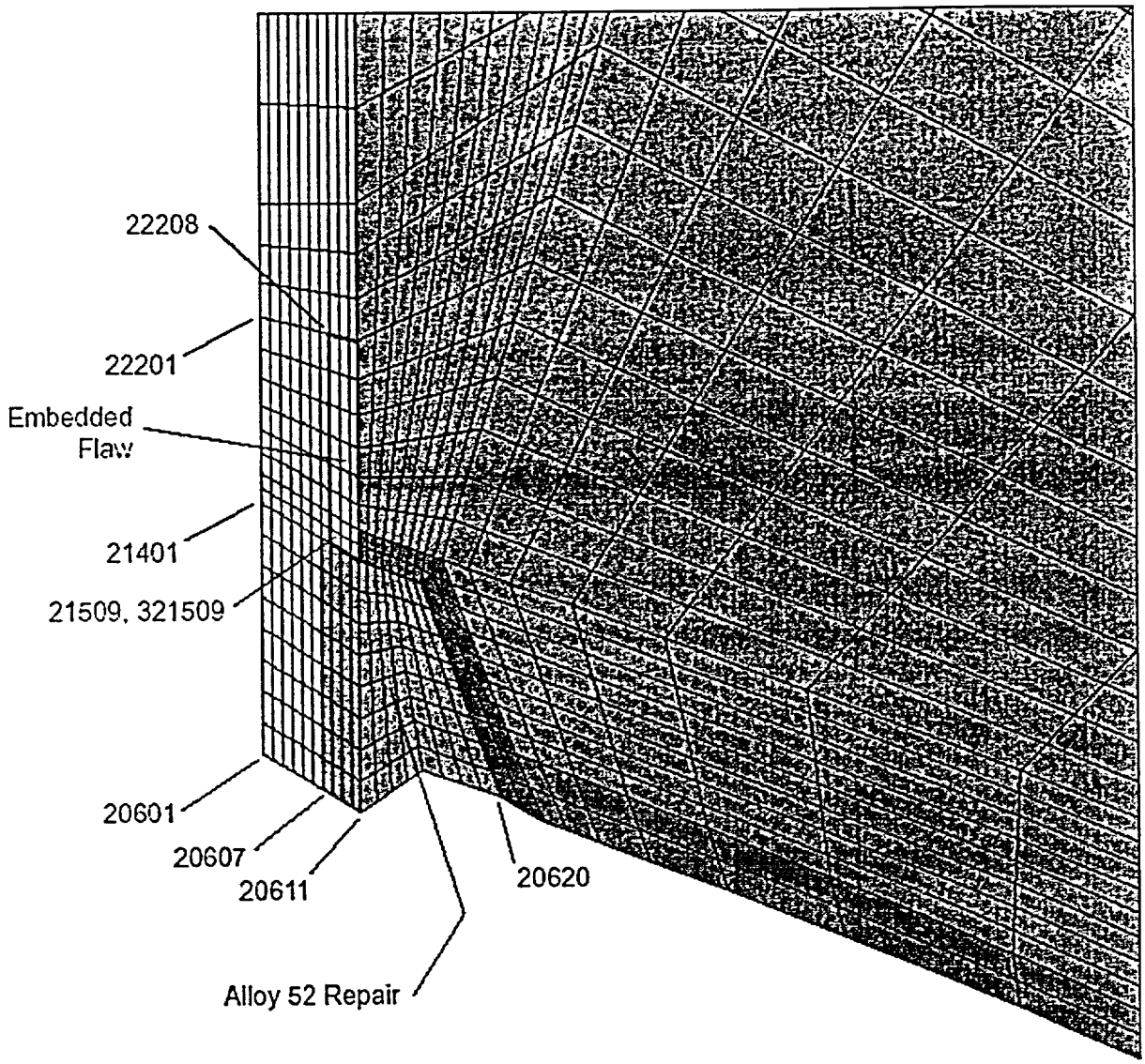

Figure A-1

DEI Nozzle 56 Embedded Flaw Model at Center of Repair Zone

(Oriented 45° from the Downhill Position)

Table A-1
Operating Hoop Stresses at 45° Plane in Unrepaired Nozzle

Penetration angle = 38.5 degrees
Nozzle yield strength = [ ] ksi

File: ANO1-38B.results.txt [3]
Time: 7007

Node	Global Coordinates X (in.)	Global Coordinates Z (in.)	ΔS[1] (in.)	Location	Hoop Stress (psi)	Distance into Head (in.)
20606	2.0000	66.306	0.000	Inside Surface of Weld	[	
20708	2.1075	66.531	0.249	Weld		
20808	2.1013	66.686	0.393	Weld		
20909	2.1901	66.873	0.598	Weld		
21010	2.2665	67.034	0.775	Weld		
21111	2.3303	67.169	0.924	Weld		
21212	2.3781	67.253	1.020	Weld		
21313	2.4170	67.336	1.111	Weld		
21415	2.5110	67.388	1.197	Weld/Butter Interface		
21516	2.5675	67.488	1.311	Butter		
21617	2.6216	67.588	1.425	Butter/Head Interface		0.000
21717	2.7462	67.743	1.619	Head		0.194
21817	2.8927	67.926	1.850	Head		0.425
21917	3.0650	68.140	2.121	Head		0.696
22017	3.2675	68.392	2.441	Head		1.016
22117	3.5057	68.688	2.818	Head		1.393
22217	3.7856	69.037	3.263	Head		1.838
22317	4.1148	69.446	3.786	Head		2.361
22417	4.5018	69.928	4.402	Head		2.977
22517	4.9568	70.494	5.127	Head		3.702
22617	5.4917	71.160	5.979	Head		4.555
22717	6.1206	71.942	6.982	Head		5.557
22817	6.8600	72.862	8.161	Head	]	6.736

[1] Distance from inside corner (node 20606*)

* Node 20606 is located on the 45° plane at the same relative position as node 606 in Figure 4.

Table A-2
Operating Hoop Stresses at 45° Plane in Repaired Nozzle 56

Penetration angle = 38.5 degrees
Nozzle yield strength = [ ] ksi

File: Noz56.flawplane.results.out [13]
Time: 12001

Node	Global Coordinates X (in.)	Global Coordinates Z (in.)	ΔS[1] (in.)	Location	Hoop Stress (psi)	Distance into Head (in.)
20611	2.0000	66.291	0.000	Inside Surface of Weld	[	
20713	2.0903	66.543	0.268	Weld		
20813	2.0843	66.730	0.447	Weld		
20914	2.1564	66.951	0.678	Weld		
21015	2.2164	67.151	0.887	Weld		
21116	2.2642	67.330	1.072	Weld		
21217	2.3067	67.462	1.210	Weld		
21318	2.3303	67.600	1.350	Weld		
21420	2.3828	67.726	1.485	Weld/Butter Interface		
21521	2.4576	67.777	1.555	Butter		
21622	2.5167	67.869	1.660	Butter/Head Interface		0.000
21722	2.5952	68.119	1.922	Head		0.262
21822	2.6805	68.392	2.208	Head		0.548
21922	2.7733	68.688	2.519	Head		0.858
22022	2.8741	69.010	2.856	Head		1.196
22122	2.9838	69.361	3.224	Head		1.563
22222	3.1030	69.742	3.623	Head		1.963
22322	3.2327	70.156	4.057	Head		2.396
22422	3.3736	70.606	4.528	Head		2.868
22522	3.5268	71.096	5.042	Head		3.381
22622	3.6934	71.628	5.599	Head		3.939
22722	3.8745	72.206	6.205	Head		4.544
22822	4.0715	72.835	6.864	Head	]	5.204

[1] Distance from inside corner (node 20611) - see Figure A-1.

Figure A-2. Operating Hoop Stresses at 45° Plane in Unrepaired Nozzle

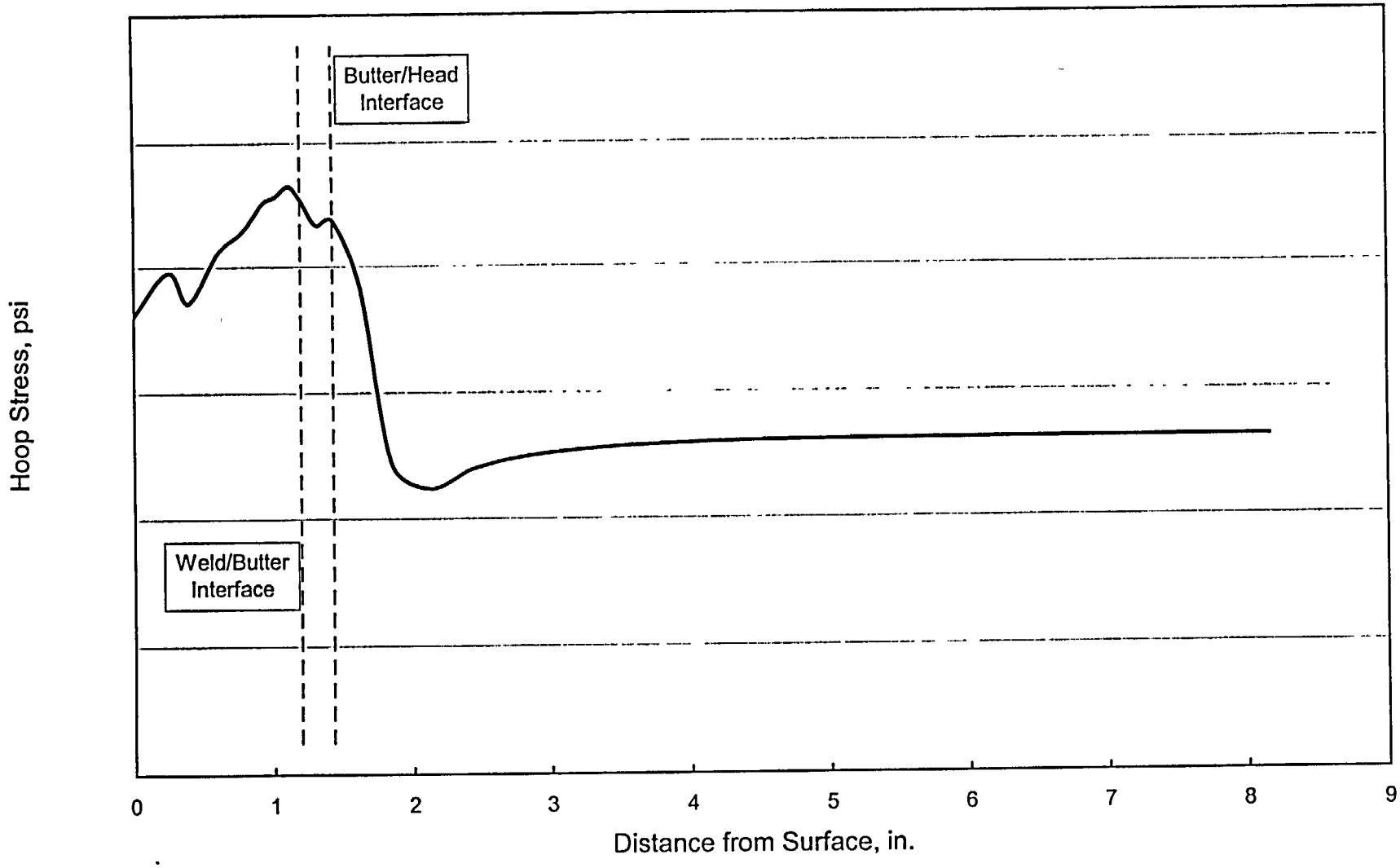

Figure A-3. Operating Hoop Stresses at 45° Plane In Repaired Nozzle 56

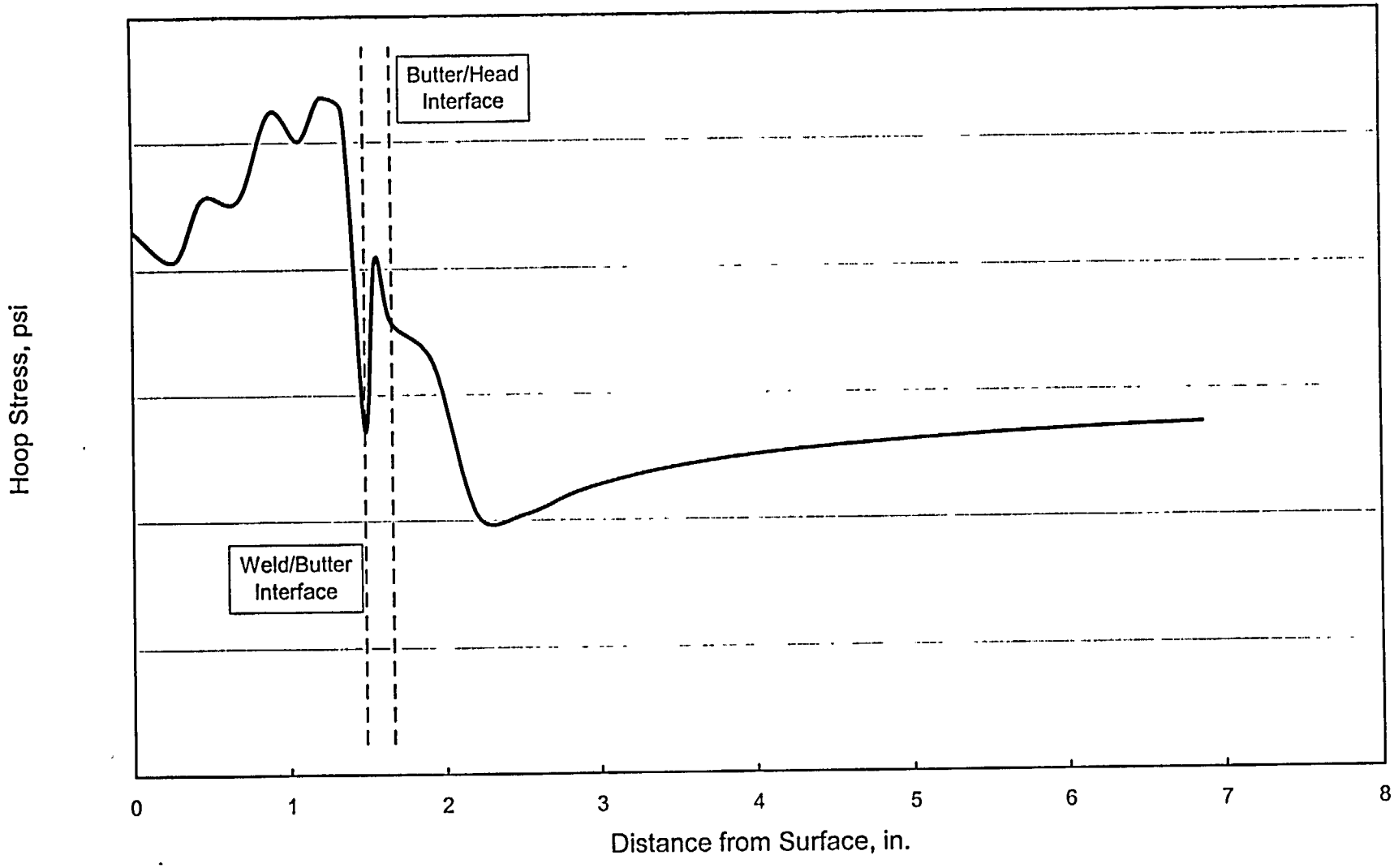

Table A-3
Operating Hoop Stresses at 45° Plane

Penetration angle = 38.5 degrees
Nozzle yield strength = [ ] ksi

Relative Nodal Position	Location	Unrepaired Nozzle Node Number	Unrepaired Nozzle Hoop Stress (psi)	Repaired Nozzle 56 Node Number	Repaired Nozzle 56 Hoop Stress (psi)
0	Inside Surface of Weld	20606	[ ]	20611	[ ]
1	Weld	20708		20713	
2	Weld	20808		20813	
3	Weld	20909		20914	
4	Weld	21010		21015	
5	Weld	21111		21116	
6	Weld	21212		21217	
7	Weld	21313		21318	
8	Weld/Butter Interface	21415		21420	
9	Butter	21516		21521	
10	Butter/Head Interface	21617		21622	
11	Head	21717		21722	
12	Head	21817		21822	
13	Head	21917		21922	
14	Head	22017		22022	
15	Head	22117		22122	
16	Head	22217		22222	
17	Head	22317		22322	
18	Head	22417		22422	
19	Head	22517		22522	
20	Head	22617		22622	
21	Head	22717		22722	
22	Head	22817	[ ]	22822	[ ]

Figure A-4. Operating Hoop Stresses at 45° Plane

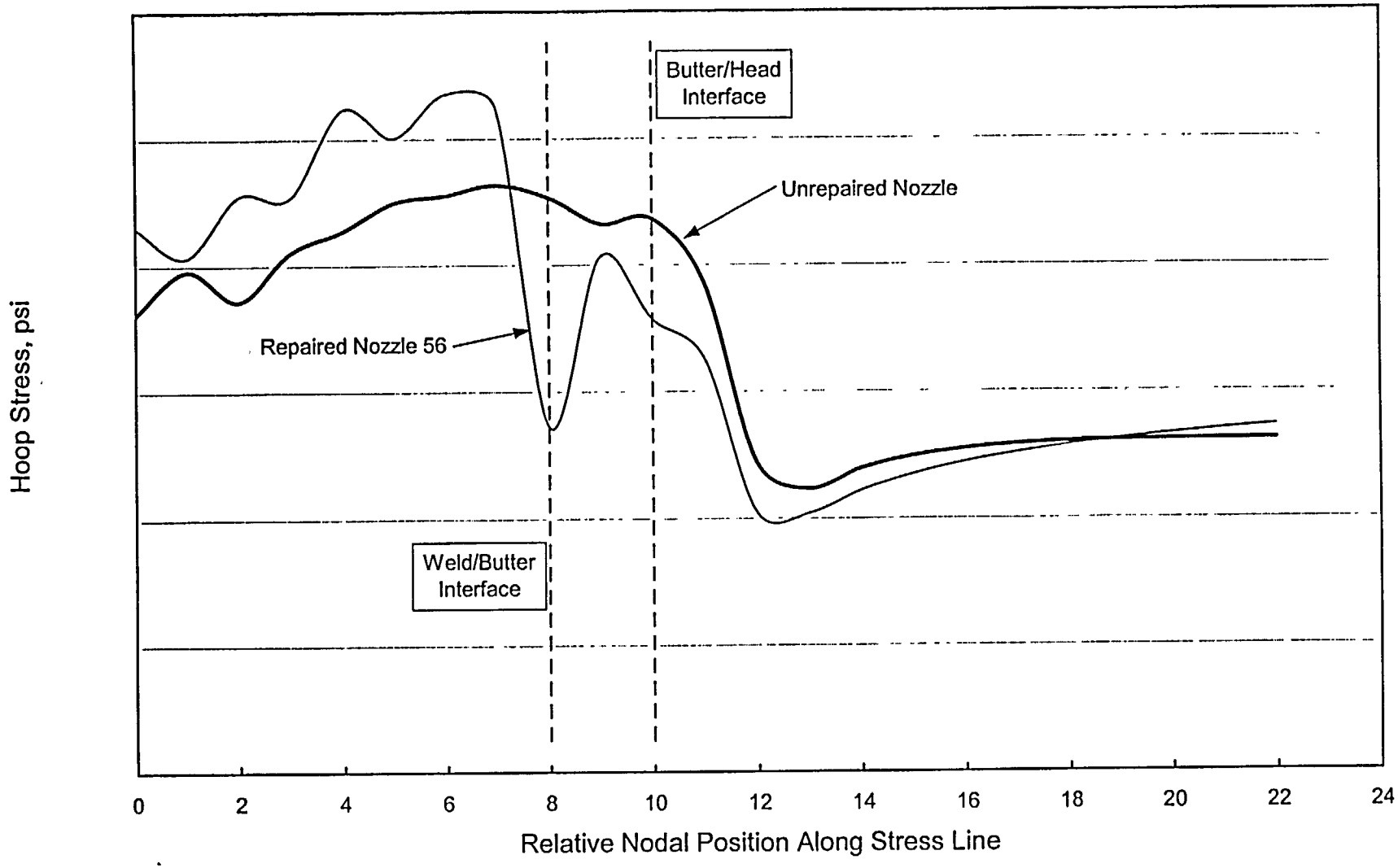

Appendix B

Certification Document

ANO-1 CRDM NOZZLE IDTB J-GROOVE WELD FLAW EVALUATION

SHEET 1 OF 1

I certify that the flaw evaluations contained in this calculation package are evidence that the CRDM nozzle repair, as defined by Framatome ANP drawing 02-5021508E-2, meets the fracture mechanics requirements identified in Framatome ANP Document 51-5021517-01 and the ASME Boiler and Pressure Vessel Code, Section XI, 1992 Edition with no addenda, for the design transients provided in Framatome ANP Document 18-1173987-03.

Exception:

The rod withdrawal transient, identified as Transient No. 11 in the functional specification for the reactor coolant system at ANO-1 (Framatome ANP Document 18-1173987-03), is analyzed as an emergency condition transient since ANO-1 has not experienced any rod withdrawal transient transients during its plant life and the likelihood of even a single future occurrence is remote. It is even more unlikely that a CRDM nozzle would experience 25 cycles of this transient, which is a requirement for classification as an emergency event.

Attested to this date: November 8, 2002

By: N/A

Douglas E. Killian
Framatome ANP, Inc.
Nuclear Engineering Business Unit
Lynchburg, Virginia

License No. 15308
Virginia Board for Architects,
Professional Engineers,
Land Surveyors,
Certified Interior Designers,
and Landscape Architects

Appendix C

Letter from Entergy for Reactor Trip Transients

32-5021538-01

ARKANSAS NUCLEAR ONE
GENERATION SUPPORT BUILDING
1448 S. R. 333
RUSSELLVILLE, AR 72801

FAX COVERLETTER

DATE 11/8/02

TO Steve Son

COMPANY NAME Framatome - ANP

CITY, STATE

FAX NUMBER VERIFY

NUMBER OF PAGES INCLUDING COVER

FROM Raymond To

COMPANY NAME Entergy

DEPARTMENT

FAX NUMBER (501) 858-4955 VERIFY (501) 858-4302

COMMENTS See attached 1 page

TO BE COMPLETED BY SENDER
AFTER TRANSMISSION IS COMPLETE, PLEASE
RETURN BY MAIL____ DISCARD____ CALL FOR PICK-UP
PHONE NUMBER_____

32-5021538-01

Steve:

Based on a review performed by our System Engineering, as documented in our ER-ANO-2001-0230-024, ANO-1 has not had a "high pressure, rod withdrawal accident" as described in transient No. 11 of RCS Functional Specification 18-1173987-03. See below for details.

++

From: MEANS, BRACY E
Sent: Friday, November 08, 2002 11:20 AM
To: TO, RAYMOND M; BAUMAN, DAVID N; CHISUM, MICHAEL R; DAIBER, BRYAN J; CHADBOURN, HARMON C; GRAY, BRIAN C; LEWIS, RAYMOND S
Subject: Reactor Trip Transients

Raymond,

The RCS Functional Specification Transient 11 (Rod Withdrawal Accident (upset condition) defines this condition as follows:
"The rod withdrawal accident occurs when one group of control rods is accidentally withdrawn from the core at the maximum rate when the reactor is operating at a low power. This transient is assumed to occur when the reactor is operating at 15% power. This causes a rapid rise in power and a reactor trip."
In an effort to facilitate transient cycle counting, FTI performed a review of the functional specification transients and consolidated the above transient in what is currently tracked as Transient #19. This FTI report has been filed as Engineering Report 95R-1015-01 and is FTI document number 51-1235146-01. In the FTI report, ANO historical transients though the year 1995 were reviewed and consolidated to reflect the current transient cycle recording document reflected in Procedure 1010.010. The transient cycle log procedure 1010.010 currently records reactor trip transients for the following conditions:

- Transient 17 - Reactor Trips with loss of RC flow. There have been 10 recorded transients in this category.
- Transient 18 - Reactor Trips with Post Overcooling. There have been 0 transients recorded in this category. The 5/18/1996 trip did not meet the overcooling requirements to be recorded in this category. It was captured in transient 19.
- Transient 19 - All Other Reactor Trips. There have been 96 recorded transients in this category through December 31, 2001. There were two RPS high pressure trips recorded. These high pressure trips did not cause a Pressurizer Code Safety valve relief with set point of 2500 psi.

The control room logs were reviewed in Autolog as well as PCRS with the plant computer data to assess related trips that may have met the criteria for Functional Specification Transient #11. **Based on this level of review, it can be stated that ANO-1 has not experienced any of the Functional Specification transient #11 events since commercial operation.** Please be advised that the transients associated with plant performance for the 2002 operating year have not been finalized. However, it is certain that none of the Functional Specification Transient #11 conditions have been experienced for ANO-1 for this year. Please advise if there are any clarifications required for the data provided herewith or if any additional input or research is desired.

Bracy

++

Raymond M. To 11/8/02

Entergy

ANO-Design Engineering Structural Group

ENCLOSURE 2

CNRO-2002-00058

FRAMATOME DOCUMENT 32-5021539
(ANO CALCULATION 86-E-0074-161)

FRAMATOME ANP

CALCULATION SUMMARY SHEET (CSS)

Document Identifier 32 - 5021539 - 01

Title ANO-1 CRDM NOZZLE IDTB WELD ANOMALY FLAW EVALUATIONS

PREPARED BY:			REVIEWED BY:		
			METHOD. ☒ DETAILED CHECK ☐ INDEPENDENT CALCULATION		
NAME	D.E. KILLIAN		NAME	A.D. NANA	
SIGNATURE			SIGNATURE		
TITLE	ADVISORY ENGR.	DATE 12/9/02	TITLE	PRINCIPAL ENGR.	DATE 12/9/02
COST CENTER	41026	REF. PAGE(S) 40,41	TM STATEMENT: REVIEWER INDEPENDENCE	ADM	

PURPOSE AND SUMMARY OF RESULTS:

Revision 1: This revision is a non-proprietary version of Revision 0.

The purpose of this analysis is to perform a fracture mechanics evaluation of a postulated anomaly in the ANO Unit 1 CRDM nozzle ID temper bead weld. This anomaly is assumed to be a [ ] inch semi-circular flaw extending 360 degrees around the circumference at the "triple point" location where there is a confluence of three materials; the Alloy 600 nozzle, the Alloy [ ] weld, and low alloy steel head. Two potential flaw propagation paths are considered in the flaw evaluations. The analysis includes prediction of fatigue crack growth in an air environment since the anomaly is located on the outside surface of the new weld, just below the bottom of the severed nozzle. Flaw acceptance is based on the 1992 ASME Code Section XI criteria for applied stress intensity factor (IWB-3612) and limit load (IWB-3642).

The results of the analysis demonstrate that the [ ] inch weld anomaly is acceptable for a 25 year design life of the CRDM nozzle ID temper bead weld repair. Significant fracture toughness margins have been demonstrated for each of the two flaw propagation paths considered in the analysis. The minimum fracture toughness margin is 4.58, compared to the required margins of $\sqrt{10}$ for normal/upset conditions and $\sqrt{2}$ for emergency/faulted conditions per IWB-3612. Fatigue crack growth is minimal since the maximum final flaw size is less than 0.101 inch. The margin on limit load is 9.44 for normal/upset conditions and 6.67 for emergency/faulted conditions, compared to the required margins of 3.0 and 1.5, respectively, per IWB-3642.

THE FOLLOWING COMPUTER CODES HAVE BEEN USED IN THIS DOCUMENT:		THE DOCUMENT CONTAINS ASSUMPTIONS THAT MUST BE VERIFIED PRIOR TO USE ON SAFETY-RELATED WORK
CODE/VERSION/REV	CODE/VERSION/REV	
		☐ YES ☒ NO

RECORD OF REVISIONS

Revision	Affected Pages	Description	Date
0	All	Original release	11/02
1	All	Revision 1 is a non-proprietary version of Revision 0.	12/02

TABLE OF CONTENTS

Section	Title	Page
1.0	INTRODUCTION	4
2.0	ASSUMPTIONS	5
3.0	WELD ANOMALY	6
4.0	MATERIAL PROPERTIES	8
5.0	APPLIED STRESSES	11
6.0	FRACTURE MECHANICS METHODOLOGY	20
7.0	ACCEPTANCE CRITERIA	22
8.0	FLAW EVALUATIONS	23
9.0	SUMMARY OF RESULTS	38
10.0	CONCLUSION	39
11.0	REFERENCES	40

Appendix	Title	Page
A	CERTIFICATION DOCUMENT	42

1.0 INTRODUCTION

The CRDM nozzle ID temper bead weld repair is described by the design drawing (Reference 1). This weld repair establishes a new pressure boundary above the original J-groove weld. The five steps involved in the repair design are listed below.

1) Roll Expansion
2) Nozzle Removal and Weld Prep Machining
3) Welding
4) Grinding/Machining and NDE
5) Remediation and Original Weld Grinding

During the welding process (step 3), a maximum [ ] inch weld anomaly may be formed due to lack of fusion at the "triple point", as shown in Figure 1. The anomaly is conservatively assumed to be a "crack-like" defect, 360 degrees around the circumference at the "triple point" location. The technical requirements document (Reference 2) provides additional details of the ID temper bead weld repair procedure. The purpose of the present fracture mechanics analysis is to provide justification, in accordance with Section XI of the ASME Code (Reference 3), for operating with the postulated weld anomaly at the triple point. Predictions of fatigue crack growth are based on a design life of 25 years.

2.0 ASSUMPTIONS

Listed below are assumptions that are pertinent to the present fracture mechanics evaluation.

1) The anomaly is assumed to include a "crack-like" defect, located at the triple-point location and extending all the way around the circumference. For analytical purposes, a continuous circumferential flaw is located in the horizontal plane at the top of the weld. Another continuous flaw is located in the cylindrical plane between the weld and reactor vessel (RV) head.

2) In the radial plane, the anomaly is assumed to include a quarter-circular "crack-like" defect (see Figure 1). For analytical purposes, a semi-circular flaw is used to represent the radial cross-section of the anomaly.

3) An RT_{NDT} value of [ ] °F is conservatively assumed for the [ ] low alloy reactor vessel head material. This is based on a highest measured value of 40 °F for 13 heats of SA-533 Grade B plate material (Reference 4).

3.0 WELD ANOMALY

The anomaly is located in the triple point region as shown in Figure 1 below.

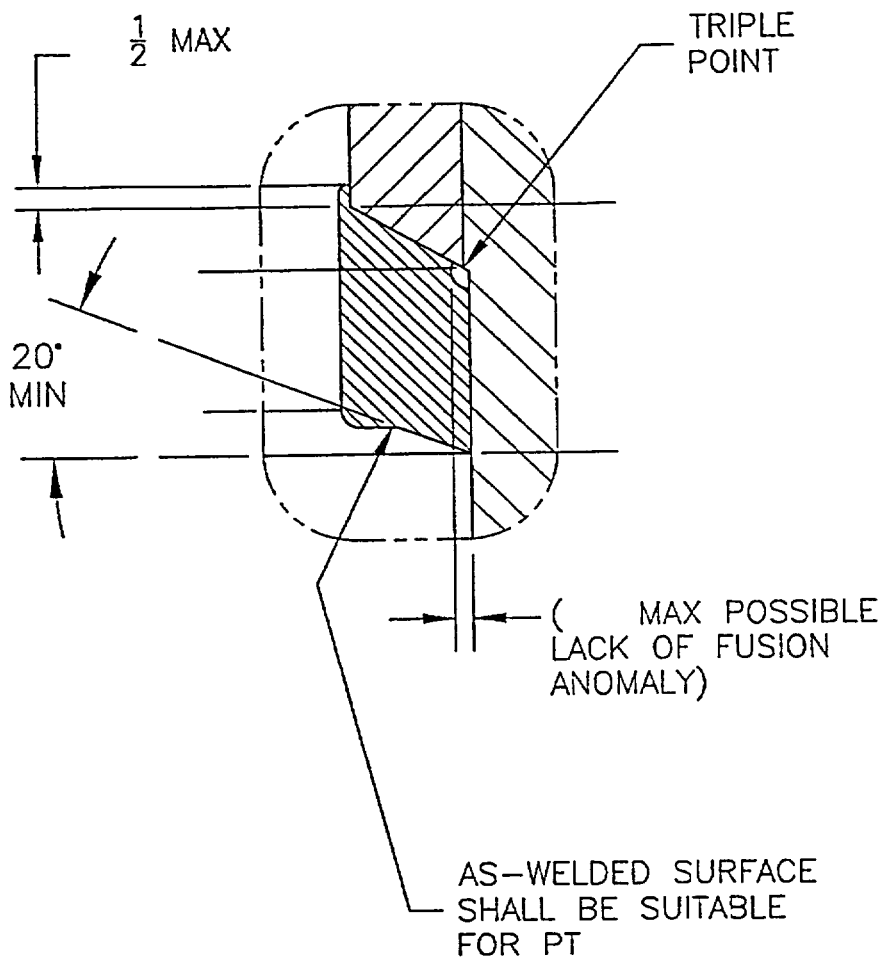

Figure 1. Weld Anomaly in Temper Bead Weld Repair

The region is called a "triple point" since three materials intersect at this location. The materials are:

a) the Alloy 600 CRDM nozzle material,

b) the new [ ] filler weld material,* and

c) the low alloy steel RV head material.

* Per Reference 7, Specification 5.14, Par. A7.4.3, "Filler metal of this classification is used for welding nickel-chromium-iron alloy (ASTM B163, B166, B167, and B168 having UNS Number [ ])." This UNS number is associated with Alloy [ ] material.

3.1 Postulated Flaws

The triple point weld anomaly is assumed to be semi-circular in shape with an initial radius of [ ]", as indicated in Figure 1. It is further assumed that the anomaly extends 360° around the nozzle. Three flaws are postulated to simulate various orientations and propagation directions for the anomaly. A circumferential flaw and an axial flaw on the outside surface of the nozzle would both propagate in a horizontal direction toward the inside surface. A cylindrically oriented flaw along the interface between the weld and head would propagate downward between the two components. The horizontal and vertical flaw propagation directions are represented in Figure 2 by separate paths for the downhill and uphill sides of the nozzle, as discussed below. For both these directions, fatigue crack growth will be calculated considering the most susceptible material for flaw propagation.

Horizontal Direction (Path 1):

Flaw propagation is across the CRDM tube wall thickness from the OD of the tube to the ID of the tube. This is the shortest path through the component wall, passing through the new Alloy [ ] weld material. However, Alloy 600 tube material properties or equivalent are used to ensure that another potential path through the HAZ between the new repair weld and the Alloy 600 tube material is bounded.

For completeness, two types of flaws are postulated at the outside surface of the tube. A 360° continuous circumferential flaw, lying in a horizontal plane, is considered to be a conservative representation of crack-like defects that may exist in the weld anomaly. This flaw would be subjected to axial stresses in the tube. An axially oriented semi-circular outside surface flaw is also considered since it would lie in a plane that is normal to the higher circumferential stresses. Both of these flaws would propagate toward the inside surface of the tube.

Vertical Direction (Path 2):

Flaw propagation is down the outside surface of the repair weld between the weld and RV head. A continuous surface flaw is postulated to lie along this cylindrical interface between the two materials. This flaw, driven by radial stresses, may propagate along either the new Alloy [ ] weld material or the low alloy steel head material.

4.0 MATERIAL PROPERTIES

The region of interest for the present flaw evaluations is at the triple point, where three different materials intersect. These materials are the CRDM nozzle material, the new weld material and the reactor vessel head material.

The ANO Unit 1 CRDM nozzles are made from Alloy 600 material to ASME specification SB-167 for tubular products (Reference 2). The new weld, as noted in Section 3.0, is made from Alloy [ ] type material. The portion of the reactor vessel head that contains the CRDM nozzles is fabricated from [ ] (Reference 2).

4.1 Yield Strength

Values of yield strength, S_y, are obtained from the 1989 Edition of the ASME Code (Reference 9), as listed below.

[ ] Low Alloy Steel Plate Material (RV Head)

Room temperature	50.0 ksi
Operating temperature of 600 °F	43.8 ksi

SB-163 Material [ ] (used for Alloy [ ] Weld Metal)

Room temperature	40.0 ksi
Operating temperature of 600 °F	31.1 ksi

SB-167 Material N06600 (Alloy 600 Material)

Room temperature	35.0 ksi
Operating temperature of 600 °F	27.9 ksi

4.2 Fracture Toughness

4.2.1. Low Alloy Steel RV Head Material

Fracture toughness curves for [ ] material are illustrated in Figure A-4200-1 of Reference 3. At an operating temperature of about 600 °F, the K_{Ia} and K_{Ic} fracture toughness values for this material (using an assumed RT_{NDT} of [ ] °F) are above 200 ksi√in. An upper bound value of 200 ksi√in will be conservatively used for the present flaw evaluations.

4.2.2. Alloy 600 and Alloy [ ] Materials

In Table 7 of Reference 12, Mills provides fracture toughness data for unirradiated Alloy 600 material at 24 °C (75 °F) and 427 °C (800 °F) in the form of crack initiation values for the J-integral, J_c. Using linear interpolation and the LEFM plane strain relationship between J_c and fracture toughness, K_{Jc},

$$K_{Jc} = \sqrt{\frac{J_c E}{1-\nu^2}},$$

the fracture toughness at an operating temperature of 600 °F is derived as follows:

Note: $\nu = 0.3$
1 kN/m = 1 kN/m ÷ 4.448 N/lb × 0.0254 m/in = 0.00571 kip/in

Temp. (F)	Mills [12] J_c (kN/m)	J_c (kip/in)	Code [9] E (ksi)	K_{Jc} (ksi√in)
75	382	2.18	31000	273
600	522	2.98	28700	307
800	575	3.28	27600	316

Since brittle fracture is not a credible failure mechanism for ductile materials like Alloy 600 or Alloy [ ], these fracture toughness measures, provided for information only, are not considered in the present flaw evaluations. However it should be noted that the fracture toughness measures of these ductile materials is significantly greater than the fracture toughness measure of the low alloy RV head material reported in Section 4.2.1. The failure mechanism for the ductile Alloy 600 and [ ] materials is limit load.

4.3 Fatigue Crack Growth

Flaw growth due to fatigue is characterized by

$$\frac{da}{dN} = C_o(\Delta K_I)^n ,$$

where C_o and n are constants that depend on the material and environmental conditions, ΔK_I is the range of applied stress intensity factor in terms of ksi√in, and da/dN is the incremental flaw growth in terms of inches/cycle. For the embedded weld anomaly considered in the present analysis, it is appropriate to use crack growth rates for an air environment. Fatigue crack growth is also dependent on the ratio of the minimum to the maximum stress intensity factor; i.e.,

$$R = (K_I)_{min} / (K_I)_{max}$$

[ ] Low Alloy Steel Plate Material (RV Head)

From Article A-4300 of the 1992 Edition of Section XI (Reference 3), the fatigue crack growth constants for subsurface flaws in an air environment are:

$$n = 3.07$$

$$C_o = 1.99 \times 10^{-10} S$$

where $S = 25.72 (2.88 - R)^{-3.07}$ for $0 \le R < 1$

Alloy 600 and Alloy [ ] Materials (used for Alloy [ ] Weld Metal)

Fatigue crack growth rates for austenitic stainless steels are used to conservatively predict flaw growth in the new Alloy [ ] repair weld. From Article C-3210 of the 1992 Edition of Section XI (Reference 3), the fatigue crack growth constants for subsurface flaws in an air environment are:

$$n = 3.3$$

$$C_o = C \times S$$

where $C = 10^{[-10.009 + 8.12E\text{-}4 \times T - 1.13E\text{-}6 \times T^2 + 1.02E\text{-}9 \times T^3]}$

$S = 1.0$ for $R \le 0$

$= 1.0 + 1.8R$ for $0 < R \le 0.79$

$= -43.35 + 57.97R$ for $0.79 < R < 1.0$

5.0 APPLIED STRESSES

The applied stresses are the cyclic stresses that contribute to fatigue crack growth. Incremental crack growth is based on six design heatup/cooldown cycles per year of operation. Residual stresses are also developed in the repair weld from the ID temper bead welding process that forms the new pressure boundary.

5.1 Fatigue Stresses

Fatigue stresses are obtained from the stress analysis contained in Reference 6. The maximum stresses, which occur during cooldown (at 10.004 hours into the composite heatup/cooldown transient), are combined with a zero stress at shutdown to produce a maximum cyclic load since stresses remain positive during this transient due to the dominating effect of pressure. The reactor coolant pressure at the 10.004 hour time point is [ ] psig (Reference 6). A slightly higher pressure ([ ] psia) occurs during a rod withdrawal accident, which is classified as an upset condition in the reactor coolant system functional specification (Reference 19). Since ANO-1 has not experienced any of these transients during its plant life (Reference 20), the rod withdrawal accident is analyzed as an emergency condition transient, with no contribution to fatigue crack growth. This exception to the functional specification is noted in the document certification statement contained in Appendix A. Stresses for the rod withdrawal transient will be obtained by multiplying the stresses at 10.004 hours into the composite heatup/cooldown transient by the ratio of the pressures for the two transients.

Component stresses are obtained for the two crack propagation paths outlined on the finite element model in Figure 2. Stresses for Paths 1 and 2 are obtained from Appendix D of Reference 6. Stresses are reported in a cylindrical coordinate system relative to the CRDM nozzle and include the three component stresses (axial, hoop and radial) needed to calculate mode I stress intensity factors for the various postulated flaws. These stresses, provided at four uniform increments along each path, were derived for ligament thicknesses of 0.488" for Path 1 and 1.143 inches for Path 2.

The stresses in Reference 6 apply directly to a weld thickness of 0.488". When the inside surface of the weld is finished by grinding, the thickness of the weld relative to the outside surface of the nozzle is

([ ]" – [ ]") / 2 = 0.518" (Reference 1)

Since the actual weld thickness is greater than the analyzed thickness, no adjustment will be made to the Reference 6 stresses in the present flaw evaluations.

To ensure that the bounding stresses are captured for use in the present flaw evaluations, stresses are obtained at every 45 degrees from the downhill (0°) to the uphill (180°) locations, as shown by the figure in Appendix D of Reference 6. It is concluded in that reference that the most limiting path is at the 180° uphill location. The uphill stresses are presented in Tables 1 and 2 for Paths 1 and 2, respectively.

As noted in the conclusions of Appendix F of Reference 6, stresses due to emergency/faulted conditions are bounded by the controlling normal/upset condition stresses. Therefore, the emergency/faulted condition stresses are bounded by the normal/upset condition stresses, considered above, for the fatigue crack growth analysis.

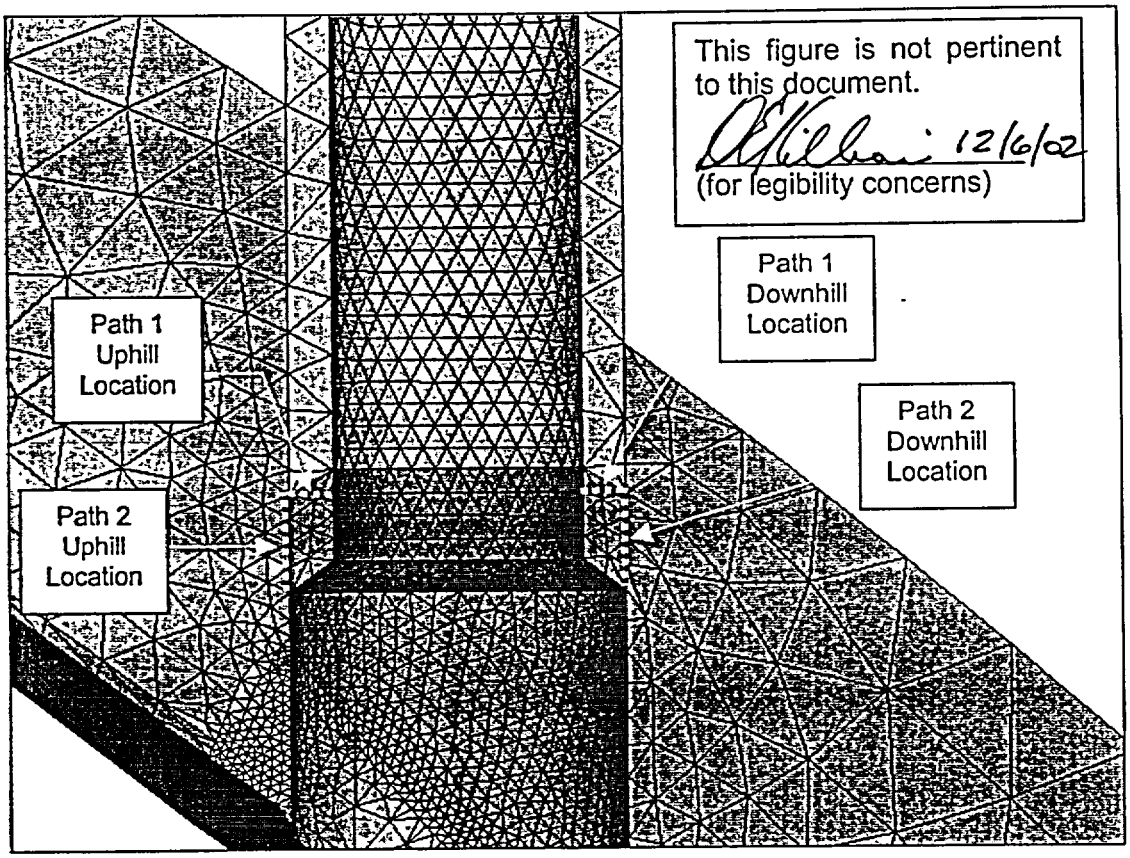

Figure 2. Illustration of Crack Propagation Paths on the Finite Element Stress Model

Table 1. Stresses for Flaw Evaluations Along Path 1 (from Reference 6)

Composite Heatup/Cooldown Transient (Normal and Upset Conditions)

Path: WA180 Length = 0.488

Pressure (psig)	Location: Time (hr.)	0.000 --SX-- Radial	0.000 --SY-- Hoop	0.000 --SZ-- Axial	0.122 --SX-- Radial	0.122 --SY-- Hoop	0.122 --SZ-- Axial	0.244 --SX-- Radial	0.244 --SY-- Hoop	0.244 --SZ-- Axial	0.366 --SX-- Radial	0.366 --SY-- Hoop	0.366 --SZ-- Axial	Triple Point 0.488 --SX-- Radial	0.488 --SY-- Hoop	0.488 --SZ-- Axial
	0.001															
	4.770															
	4.871															
	7.000															
	7.313															
	7.412															
	10.000															
	10 004															
	10.013															
	10.117															
	10.217															
	10.250															
	10.718															
	12.939															

Ratioed Stresses for Rod Withdrawl Accident (Emergency Condition)

Note: Rod Withdrawal Accident Stress = ([ ] psig / [ ] psig) * Heatup/Cooldown Stress

Pressure (psig)	Location:	0.000 --SX-- Radial	0.000 --SY-- Hoop	0.000 --SZ-- Axial	0.122 --SX-- Radial	0.122 --SY-- Hoop	0.122 --SZ-- Axial	0 244 --SX-- Radial	0.244 --SY-- Hoop	0 244 --SZ-- Axial	0.366 --SX-- Radial	0.366 --SY-- Hoop	0 366 --SZ-- Axial	Triple Point 0 488 --SX-- Radial	0.488 --SY-- Hoop	0 488 --SZ-- Axial

Legend:
SX = radial stress
SY = hoop stress
SZ = axial stress

Table 2. Stresses for Flaw Evaluations Along Path 2 (from Reference 6)

Composite Heatup/Cooldown Transient (Normal and Upset Conditions)

Path: **WV180** Length = 1.143

Pressure (psig)	Location: Time (hr.)	0 0000 --SX-- Radial	0 0000 --SY-- Hoop	0 0000 --SZ-- Axial	0.2858 --SX-- Radial	0.2858 --SY-- Hoop	0 2858 --SZ-- Axial	0.5715 --SX-- Radial	0.5715 --SY-- Hoop	0 5715 --SZ-- Axial	0 8573 --SX-- Radial	0.8573 --SY-- Hoop	0 8573 --SZ-- Axial	Triple Point 1.1430 --SX-- Radial	1.1430 --SY-- Hoop	1.1430 --SZ-- Axial
	0.001															
	4.770															
	4.871															
	7.000															
	7.313															
	7.412															
	10.000															
	10.004															
	10.013															
	10.117															
	10.217															
	10.250															
	10.718															
	12.939															

Ratioed Stresses for Rod Withdrawl Accident (Emergency Condition)

Note: Rod Withdrawal Accident Stress = ([ ] psig / [ ] psig) * Heatup/Cooldown Stress

Pressure (psig)	Location:	0.000 --SX-- Radial	0.000 --SY-- Hoop	0.000 --SZ-- Axial	0 122 --SX-- Radial	0.122 --SY-- Hoop	0.122 --SZ-- Axial	0 244 --SX-- Radial	0 244 --SY-- Hoop	0.244 --SZ-- Axial	0.366 --SX-- Radial	0 366 --SY-- Hoop	0 366 --SZ-- Axial	Triple Point 0.488 --SX-- Radial	0.488 --SY-- Hoop	0 488 --SZ-- Axial

Legend:
SX = radial stress
SY = hoop stress
SZ = axial stress

5.2 Residual Stresses

A three-dimensional elastic-plastic finite element analysis (Reference 5) was performed by Dominion Engineering, Inc. (DEI) to simulate the sequence of steps involved in arriving at the configuration of the CRDM nozzle and reactor vessel head after completion of the ID temper bead repair. To simply the analysis of the complete repair process, only the center nozzle was modeled (Figure 3). Although this axisymmetric analysis was based on the geometry of the center nozzle penetration, adjustments were made to represent significant aspects of the controlling nozzle at the outermost hillside location (38° from the top of the vessel). In particular, the repair weld was positioned at the minimum distance above the J-groove and the J-groove weld was chamfered to simulate the largest chamfer (7/8"). The model also used the highest yield strength of any nozzle in the head ([ ] ksi). The 38° nozzle location was limiting for all three of these conditions.

The DEI analysis simulated the laying of the original weld butter and the subsequent post-weld stress relief, the heatup of the original J-groove weld and adjacent material during the welding process and the subsequent cooldown to ambient temperature, a pre-service hydro test, and operation at steady state conditions. After the steady state loads were removed and the structure was again at ambient conditions, the portion of the nozzle below the cut line (Reference 1) was deleted. Deposition of the repair weld was simulated using four weld passes, and the J-groove weld was chamfered as shown in Figure 4. The analysis of this final configuration provided residual stresses in the repair weld for use in the present flaw evaluations. These stresses are listed in Table 3.

The repair weld analysis of Reference 5 used a multi-linear isotropic hardening model to characterize the nozzle material and elastic-perfectly plastic material models for the welds, butter, cladding and head. The yield strengths for the non-strain hardening models were selected to represent the flow stress of the various materials. The following yield strength values were used in the DEI repair weld analysis:

Component	Material	Yield Strength at 600 °F
Nozzle	Alloy 600	[ ] ksi
Repair weld	Alloy [ ]	[ ] ksi
J-groove weld	Alloy 182	[ ] ksi
Butter	Alloy 182	[ ] ksi
Head	Low alloy steel	[ ] ksi
Cladding	Stainless steel	[ ] ksi

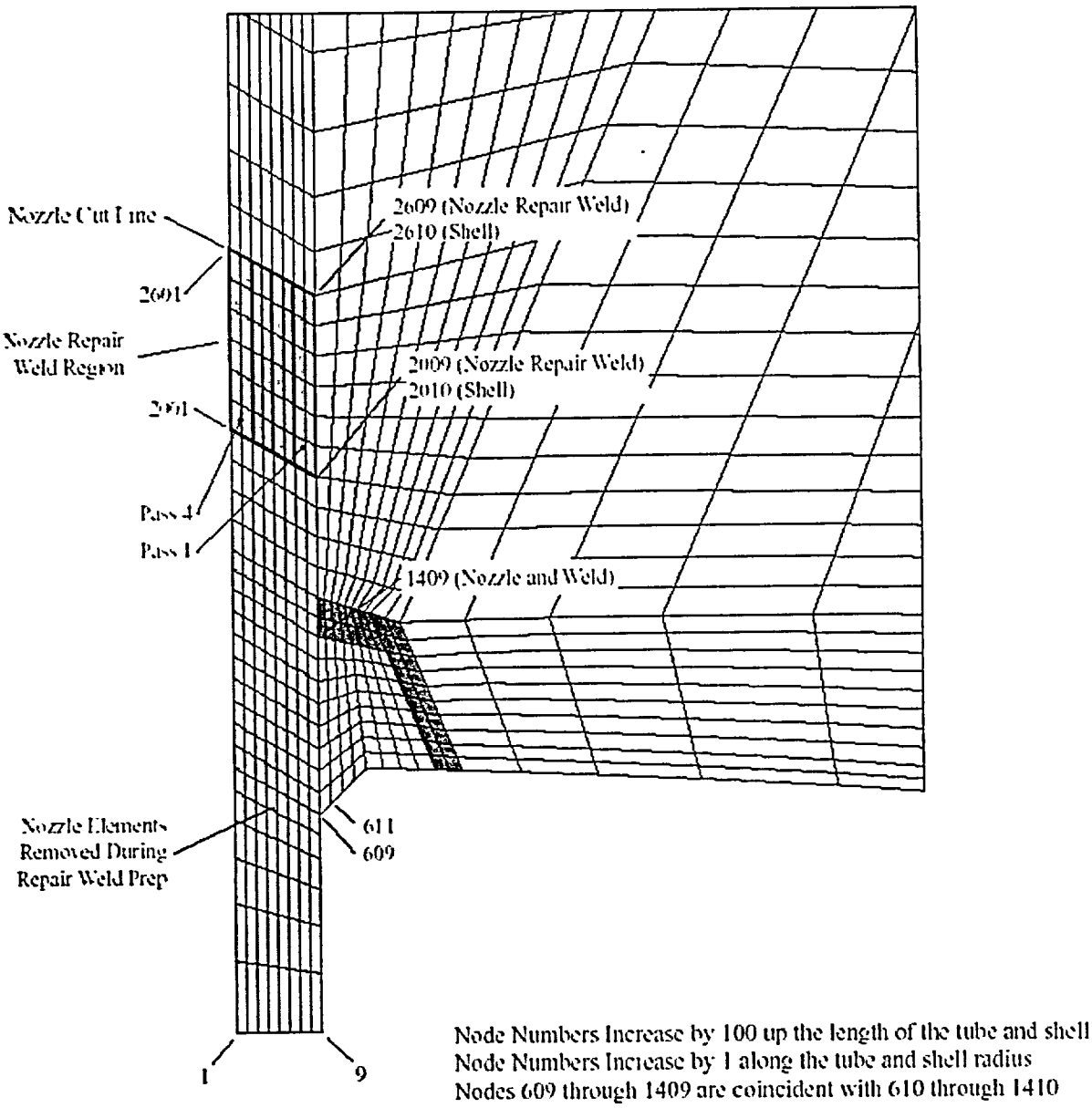

Figure 3. DEI Model for Center CRDM Nozzle with Weld Repair

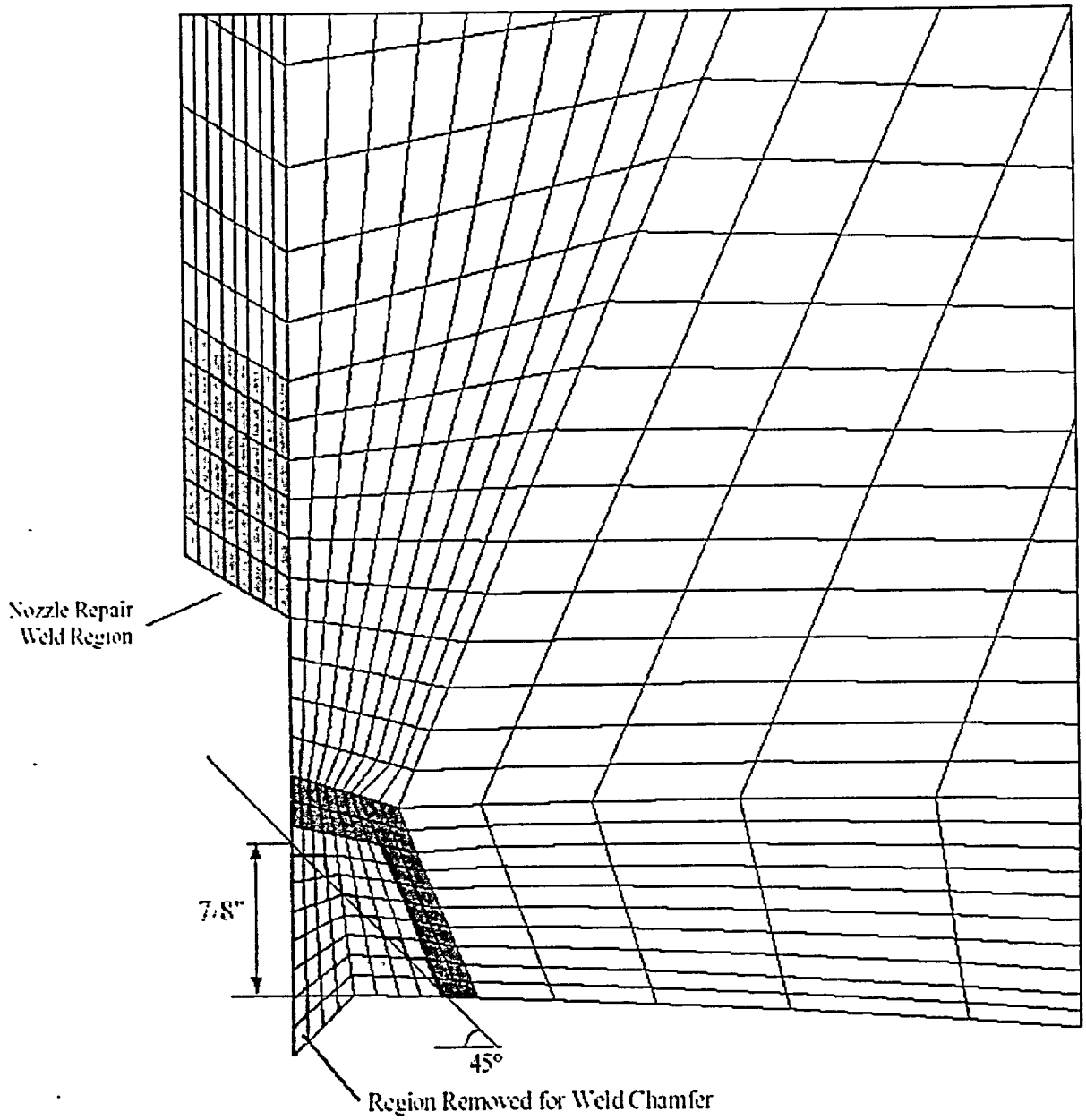

Figure 4. DEI Model for Center CRDM Nozzle After Weld Repair and Chamfer

Table 3
Residual Stresses in Repair Weld after Chamfering J-Weld

Penetration angle = 0 degrees
Nozzle yield strength = [ ] ksi

File: ANO1-0B.results.txt (Reference 5)
Time: 16001

Path Along Interface Between Repair Weld and Remaining Nozzle
(Corresponds to Path 1)

Location	Node	Radial Stress (psi)	Hoop Stress (psi)	Axial Stress (psi)	Coordinates X (in.)	Coordinates Z (in.)
Triple Point	2609	[		]	2.0000	90.525
	2608				1.9228	90.570
	2607				1.8456	90.615
	2606				1.7684	90.659
	2605				1.6912	90.704
	2604				1.6141	90.748
	2603				1.5369	90.793
	2602				1.4597	90.837
Inside Surface	2601			]	1.3825	90.882

Table 3 (Cont'd)
Residual Stresses in Repair Weld after Chamfering J-Weld

Penetration angle = 0 degrees
Nozzle yield strength = [ ] ksi

File: ANO1-0B.results.txt (Reference 5)
Time: 16001

Path Along Interface Between Repair Weld and Reactor Vessel Head
(Corresponds to Path 2)

Stresses in Weld

Location	Node	Radial Stress (psi)	Hoop Stress (psi)	Axial Stress (psi)	Coordinates X (in.)	Coordinates Z (in.)	Relative Position (in.)
Triple Point	2609	[		]	2.000	90.525	0.000
	2509				2.000	90.302	0.223
	2409				2.000	90.079	0.446
	2309				2.000	89.855	0.670
	2209				2.000	89.632	0.893
	2109				2.000	89.409	1.116
Lower End	2009			]	2.000	89.185	1.340

Stresses in Head

Location	Node	Radial Stress (psi)	Hoop Stress (psi)	Axial Stress (psi)	Coordinates X (in.)	Coordinates Z (in.)	Relative Position (in.)
Triple Point	2610	[		]	2.000	90.525	0.000
	2510				2.000	90.302	0.223
	2410				2.000	90.079	0.446
	2310				2.000	89.855	0.670
	2210				2.000	89.632	0.893
	2110				2.000	89.409	1.116
Lower End	2010			]	2.000	89.185	1.340

6.0 FRACTURE MECHANICS METHODOLOGY

This section presents several aspects of linear elastic fracture mechanics (LEFM) and limit load analysis (to address the ductile Alloy 600 and Alloy [ ] materials) that form the basis of the present flaw evaluations. As discussed in Section 3.1, flaw evaluations are performed for flaw propagation Paths 1 and 2 in Figure 2.

Path 1 represents a section across the new Alloy [ ] weld metal which is equivalent to the thickness of the CRDM tube wall. Since the weld anomaly is located at the base of the OD of the CRDM tube and is assumed to be all the way around the circumference, a stress intensity factor (SIF) solution for a 360 degree circumferential crack on the OD of a circular tube is deemed appropriate. Therefore, the SIF solution of Buchalet and Bamford (Reference 13) is used in the analysis. However, this solution is applicable to a 360-degree part-through ID flaw. To develop an SIF solution for a 360 degree part-through OD flaw, an F function is determined based on SIF solutions of Kumar (References 14 and 15). Appropriate F functions for internal and external circumferential flaws are determined for a cylinder subjected to remote tension. The ratio of the F functions for the external and internal flaws is considered to be an appropriate multiplying factor for the Buchalet and Bamford SIF solution to extend its application to an external flaw. Similar ratios have been reported by Kumar (Reference 18). The materials to be considered for this path are the Alloy 600 tube material or the Alloy [ ] weld metal. Fatigue crack growth is calculated using crack growth rates for austenitic stainless steels from Appendix C of Section XI (Reference 3). A limit load analysis for an external circumferential flaw in a cylinder subjected to remote tension (Reference 15) is also performed for applied loads on the CRDM tube.

An axially oriented semi-circular OD surface flaw is also considered in the evaluation, as illustrated by the schematic below.

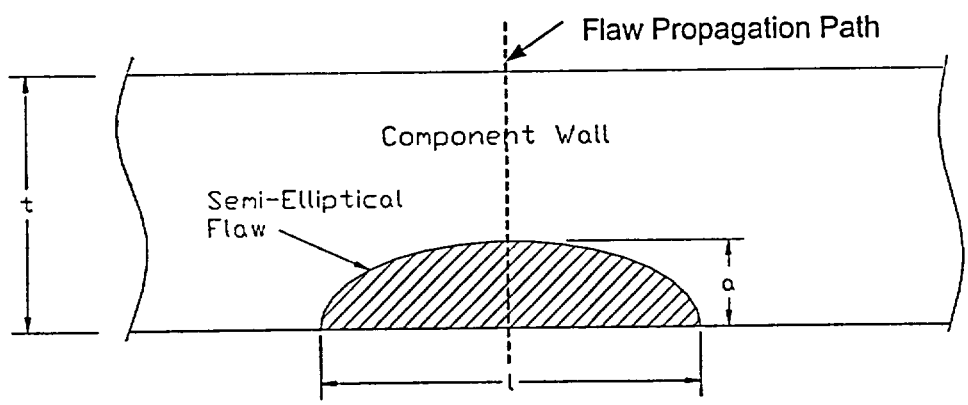

where, a = initial flaw depth = [ ] inch

l = 2c = flaw length = [ ] inch

t = wall thickness = 0.518 inch

An axial flaw is considered since the stresses in the CRDM penetration region are primarily due to pressure and therefore the hoop stresses are more significant. The SIF solution by Raju & Newman (Reference 10) for an external surface crack in a cylindrical vessel is used in the

evaluation, considering growth in both the radial and axial directions. The fatigue flaw growth analysis for the axial crack is also performed using the austenitic stainless steel crack growth rates.

The Irwin plasticity correction is also considered in the SIF solutions discussed above. This plastic zone correction is discussed in detail in Section 2.8.1 of Reference 11. The effective crack length is defined as the sum of the actual crack size and the plastic zone correction:

$$a_e = a + r_y$$

where r_y for plane strain conditions (applicable for this analysis) is given by:

$$r_y = \frac{1}{6\pi}\left(\frac{K_I}{\sigma_{YS}}\right)^2$$

Path 2 represents the interface between the new repair weld and the RV head material. The potential for flaw propagation along this interface is likely if radial stresses are significant between the weld and head. This assessment utilizes an SIF solution for a continuous surface crack in a flat plate from Appendix A of the 1995 Edition of Section XI (Reference 16). Flat plate solutions are routinely used to evaluate flaws in cylindrical components such as the repair weld since the added constraint provided by the cylindrical structure reduces the crack opening displacements. The solution is therefore inherently conservative for this application. Crack growth analysis is performed considering propagation through the Alloy [ ] weld metal or the low alloy steel head material, whichever is limiting.

7.0 ACCEPTANCE CRITERIA

The low alloy steel reactor vessel head material will be evaluated against the IWB-3612 acceptance criteria of Section XI (Reference 3). For the highly ductile materials Alloy 600 and Alloy [ ] materials, the initial flaw depth to thickness ratio for the postulated weld anomaly is only about 20% and fatigue crack growth is minimal for these materials in an air environment. A convenient acceptance criterion on flaw size is the industry developed 75% through-wall limit on depth (Reference 8):

$$\frac{a}{t} \leq 0.75$$

For the shallow cracks considered in the present analysis, this criterion is easily met. In addition, stress intensity factors will be calculated and evaluated against conservative fracture toughness requirements using a factor of safety of $\sqrt{10}$ for normal and upset conditions.

Another acceptance criterion for ductile materials is demonstration of sufficient limit load margin. From IWB-3642 (Reference 3), the required safety margin, based on load, is a factor of 3 for normal and upset conditions and a factor of 1.5 for emergency and faulted conditions.

Since stresses for emergency/faulted conditions are bounded by the controlling normal/upset condition stresses (see Section 5.0) and the required fracture toughness margins are less stringent for emergency/faulted conditions, satisfying normal/upset conditions requirements implicitly satisfies those for emergency/faulted conditions as well.

8.0 FLAW EVALUATIONS

The evaluation of the postulated external circumferential flaw for propagation along Path 1 is contained in Tables 4 and 5. The fatigue crack growth analysis is provided in Table 4 and a limit load analysis is presented in Table 5.

The evaluation of an external axial flaw for fatigue crack growth along Path 1 is contained in Table 6.

A continuous surface flaw along the cylindrical interface between the repair weld and the reactor vessel head is analyzed for fatigue crack growth along Path 2 in Table 7.

The flaw evaluations utilize the combined stresses resulting from the sum of the residual stresses from Reference 3 and the fatigue stresses from Reference 6. This is a conservative approximation of the actual state of stress since the elastic fatigue stresses are added directly to the elastic-plastic residual stresses, with no attenuation for additional plastic strain. It is therefore appropriate to use the yield strengths from the DEI stress analysis (Reference 3) when applying the Irwin plastic zone correction for crack length.

As required by Article IWB-3612 (Reference 3), a safety factor of $\sqrt{10}$ is used to evaluate applied stress intensity factors for normal and upset conditions, considering the lower K_{Ia} fracture toughness for crack arrest. Article IWB-3612 also specifies that a safety factor of $\sqrt{2}$ must be used for emergency and faulted conditions, along with the higher K_{Ic} fracture toughness for crack initiation. Since the required safety margin for the emergency condition rod withdrawal accident is less than that for normal and upset conditions by a factor of $\sqrt{10} / \sqrt{2} = 2.24$ and the rod withdrawal accident stresses from Tables 1 and 2 are only [ ] psig / [ ] psig, or 1.05 times the maximum normal and upset condition stresses, the flaw evaluations performed for normal and upset conditions serve as a bounding analysis for the emergency condition rod withdrawal accident.

Table 4. Evaluation of Continuous External Circumferential Flaw for Fatigue Crack Growth Along Path 1

INPUT DATA

Geometry:	Outside diameter,	Do =	[ ]	in.
	Inside diameter,	Di =		in.
	Thickness,	t =	0.518	in.
		Ri/t =	2.861	
Flaw Size:	Flaw depth,	a =	[ ]	in.
		a/t =		
Environment:	Temperature,	T =	600	F

Table 4. Evaluation of Continuous External Circumferential Flaw for Fatigue Crack Growth Along Path 1 (Cont'd)

Variation of F Function between Continuous External and Continuous Internal Circumferential Flaws Using Solutions by V. Kumar et al.

Source: EPRI NP-1931 Topical Report, Section 4.3 for an internal circumferential crack under remote tension (Ref. 14).

The applied KI equation is given by the expression:

$$KI = \sigma * \sqrt{(\pi * a)} * F(a/b, Ri/Ro)$$

where

$$\sigma = P/(\pi * (Ro^2 - Ri^2)$$

and F is a function of a/b and b/Ri,

where a/b = [ ]
b/Ri = [ ]

By extrapolation from Table 4-5 of EPRI-1931, the internal F-factor is estimated to be:

$F_{internal}$ = 1.14

Source: GE Report SRD-82-048, Prepared for EPRI Contract RP-1237-1, Fifth & Sixth Semi-Annual Report, Section 3.5 for an external circumferential under remote tension (Ref. 15).

For the external circumferential crack, the expressions for KI and σ are as defined above for the internal circumferential crack,

where a/b = [ ]
Ri/Ro = [ ]

From Figure 3-11 of SRD-82-048, the external F-factor is estimated to be:

$F_{external}$ = 1.25

Multiplying Factor:

To estimate the stress intensity factor for an external circumferential crack from the solution for an internal circumferential crack under remote tension, the appropriate multiplying factor is:

$$F_{external} / F_{internal} = 1.25 / 1.14 \approx 1.10$$

An alternate source for this multiplying factor is EPRI NP-3607 (Ref. 18). From Figure 3-9, the multiplying factor for circumferential flaws with an a/t ratio of 0.2 can also be estimated to be:

$$F_{external} / F_{internal} \approx 1.10$$

Table 4. Evaluation of Continuous External Circumferential Flaw for Fatigue Crack Growth Along Path 1 (Cont'd)

STRESS INTENSITY FACTOR FOR CIRCUMFERENTIAL FLAW

Basis: Buchalet and Bamford solution for continuous circumferential flaws on the inside surface of cylinders (Ref. 13)

$$KI = \sqrt{(\pi * a)} * [\, A_0 F_1 + (2a/\pi) A_1 F_2 + (a^2/2) A_2 F_3 + (4a^3)/(3\pi) A_3 F_4 \,]$$

where,

$$F1 = 1.1259 + 0.2344(a/t) + 2.2018(a/t)^2 - 0.2083(a/t)^3$$
$$F2 = 1.0732 + 0.2677(a/t) + 0.6661(a/t)^2 + 0.6354(a/t)^3$$
$$F3 = 1.0528 + 0.1065(a/t) + 0.4429(a/t)^2 + 0.6042(a/t)^3$$
$$F4 = 1.0387 - 0.0939(a/t) + 0.6018(a/t)^2 + 0.3750(a/t)^3$$

and the through-wall stress distribution is described by the third order polynomial,

$$S(x) = A_0 + A_1 x + A_2 x^2 + A_3 x^3.$$

Applicablility: $Ri/t = 10$
$a/t \leq 0.8$

Axial Stresses:

Wall Position x	Residual Stress in Weld	Normal/Upset Cond. Stresses [6]		Total Stresses at Operation	
		Cooldown	Shutdown	Cooldown	Shutdown
(in.)	(ksi)	(ksi)	(ksi)	(ksi)	(ksi)
0.00000					
0.12950					
0.25900					
0.38850					
0.51800					

Stress Coefficients:

Stress Coeff.	Normal/Upset Loading Conditions	
	NU1	NU2
	(ksi)	(ksi)
A_0		
A_1		
A_2		
A_3		

Table 4, Evaluation of Continuous External Circumferential Flaw for Fatigue Crack Growth Along Path 1 (Cont'd)

CRACK GROWTH FOR CIRCUMFERENTIAL FLAW (IN-AIR) - AUSTENITIC MATERIAL

Basis: $\Delta a = \Delta N * C_o(\Delta KI)^n$ $\Delta N =$ 6 fatigue cycles / year Sy = 27.9 ksi

Operating Time (yr.)	Cycle	a (in.)	NU1 KI(a)max (ksi√in)	NU2 KI(a)min (ksi√in)	ΔKI (ksi√in)	R	S	C_o	Δa (in.)	r_y	a_e	NU1 KI(a_e)max (ksi√in)
0	0		-18.01	-35.63	17.62	0.00	1.00	1.96E-10	1.52E-05	0.0212		-21.50
1	6		-18.01	-35.64	17.62	0.00	1.00	1.96E-10	1.52E-05	0.0212		-21.51
2	12		-18.01	-35.64	17.62	0.00	1.00	1.96E-10	1.52E-05	0.0212		-21.51
3	18		-18.02	-35.64	17.63	0.00	1.00	1.96E-10	1.52E-05	0.0212		-21.51
4	24		-18.02	-35.65	17.63	0.00	1.00	1.96E-10	1.52E-05	0.0212		-21.51
5	30		-18.02	-35.65	17.63	0.00	1.00	1.96E-10	1.52E-05	0.0212		-21.52
6	36		-18.03	-35.65	17.63	0.00	1.00	1.96E-10	1.52E-05	0.0212		-21.52
7	42		-18.03	-35.66	17.63	0.00	1.00	1.96E-10	1.52E-05	0.0212		-21.52
8	48		-18.03	-35.66	17.63	0.00	1.00	1.96E-10	1.52E-05	0.0212		-21.52
9	54		-18.03	-35.66	17.63	0.00	1.00	1.96E-10	1.52E-05	0.0212		-21.53
10	60		-18.04	-35.67	17.63	0.00	1.00	1.96E-10	1.52E-05	0.0212		-21.53
11	66		-18.04	-35.67	17.63	0.00	1.00	1.96E-10	1.52E-05	0.0212		-21.53
12	72		-18.04	-35.68	17.63	0.00	1.00	1.96E-10	1.52E-05	0.0212		-21.53
13	78		-18.04	-35.68	17.64	0.00	1.00	1.96E-10	1.52E-05	0 0212		-21.54
14	84		-18.05	-35 68	17.64	0.00	1.00	1.96E-10	1.52E-05	0.0212		-21.54
15	90		-18.05	-35.69	17.64	0.00	1.00	1.96E-10	1.52E-05	0.0212		-21.54
16	96		-18.05	-35.69	17.64	0.00	1.00	1.96E-10	1.52E-05	0.0212		-21.55
17	102		-18.05	-35.69	17.64	0.00	1.00	1.96E-10	1.52E-05	0.0212		-21.55
18	108		-18.06	-35.70	17.64	0.00	1.00	1.96E-10	1.53E-05	0.0212		-21.55
19	114		-18.06	-35.70	17.64	0.00	1.00	1.96E-10	1.53E-05	0.0212		-21.55
20	120		-18.06	-35.70	17.64	0.00	1.00	1.96E-10	1.53E-05	0.0212		-21.56
21	126		-18.07	-35.71	17.64	0.00	1.00	1.96E-10	1.53E-05	0.0212		-21.56
22	132		-18.07	-35.71	17.64	0.00	1.00	1.96E-10	1.53E-05	0.0212		-21.56
23	138		-18.07	-35.72	17.64	0.00	1.00	1.96E-10	1.53E-05	0.0212		-21.56
24	144		-18.07	-35.72	17.65	0.00	1.00	1.96E-10	1.53E-05	0.0212		-21.57
25	150		-18.08	-35.72	17.65	0.00	1.00	1.96E-10	1.53E-05	0.0212		-21.57

Table 5. Limit Load Analysis for a Continuous External Circumferenital Flaw

LIMIT LOAD

Basis: GE Report SRD-82-048, Combined Fifth and Sixth Semi-Annual Report by V. Kumar et al, Section 3.5 (Ref. 15).

For remote tension loading,

$$Po = 2/\sqrt{3}*\sigma_o*\pi*(Rc^2-Ri^2)$$

where

$$Rc = Ro - a$$

and

σ_o = 27900 psi (conservatively using the minimum yield strength)

Ro = [ ] in.

a = [ ] in.

Rc = [ ] in.

Ri = [ ] in.

Then

Po = [ ] lbs

From Reference 17, the applied loads on a typical B&W design CRDM tube are:

a) Normal/Upset conditions, P = [ ] lbs

b) Emergency/Faulted conditions, P = [ ] lbs

The limit load margins are greater than those required by Article IWB-3642 of Section XI (Ref. 3), as shown below.

a) Normal/Upset conditions,	Po/P =	9.44	> 3.0
b) Emergency/Faulted conditions,	Po/P =	6.67	> 1.5

Table 6. Evaluation of an External Axial Flaw for Fatigue Crack Growth Along Path 1

INPUT DATA

Geometry:	Outside diameter,	Do =	[ ]	in.
	Inside diameter,	Di =		in.
	Thickness,	t =	0.518	in.
		Ri/t =	2.861	
Flaw Size:	Flaw depth,	a =	[ ]	in.
	Flaw length,	ℓ =		in.
		a/t =		
Environment:	Temperature,	T =	600	F

Table 6. Evaluation of an External Axial Flaw for Fatigue Crack Growth Along Path 1 (Cont'd)

STRESS INTENSITY FACTOR FOR AXIAL FLAW

Basis: Raju & Newman, "Stress Intensity Factors for Internal & External Surface Cracks in Cylindrical Vessels (Ref. 10)

$$KI = \sqrt{(\pi/Q)} * [G_0 A_0 a^{0.5} + G_1 A_1 a^{1.5} + G_2 A_2 a^{2.5} + G_3 A_3 a^{3.5}]$$

where, from Table 4 of Reference 10, for an external surface crack with t/R = 0.25, a/t = 0.2, a/c = 1.0, the influence coefficients are as follows:

Location:	Deepest Point ($2\phi/\pi = 1$)	Surface ($2\phi/\pi = 0$)
Go =	1.030	1.163
G_1 =	0.720	0.204
G_2 =	0.591	0.077
G_3 =	0.513	0.040

and Q = 2.464 = (1 + 1.464*(a/c)^1.65)

and the through-wall stress distribution is described by the third order polynomial,

$$S(x) = A_0 + A_1 x + A_2 x^2 + A_3 x^3.$$

Hoop Stresses:

Wall Position x	Residual Stress in Weld	Normal/Upset Cond. Stresses [6]		Total Stresses at Operation	
		Cooldown	Shutdown	Cooldown	Shutdown
(in.)	(ksi)	(ksi)	(ksi)	(ksi)	(ksi)
0.00000					
0.12950					
0.25900					
0.38850					
0.51800					

Stress Coefficients:

Stress Coeff.	Normal/Upset Loading Conditions	
	NU1	NU2
	(ksi)	(ksi)
A_0		
A_1		
A_2		
A_3		

Table 6. Evaluation of an External Axial Flaw for Fatigue Crack Growth Along Path 1 (Cont'd)

RADIAL CRACK GROWTH FOR AXIAL FLAW (IN-AIR) - AUSTENITIC MATERIAL

Basis: $\Delta a = \Delta N * C_o(\Delta KI)^n$ $\Delta N =$ 6 fatigue cycles / year Sy = 42.5 ksi

Operating Time (yr.)	Cycle	a (in.)	NU1 KI(a)max (ksi√in)	NU2 KI(a)min (ksi√in)	ΔKI (ksi√in)	R	S	C_o	Δa (in.)	r_y	a_e	NU1 KI(a_e)max (ksi√in)
0	0		25.80	9.19	16.62	0.36	1.64	3.21E-10	2.06E-05	0.0196		28.72
1	6		25.81	9.19	16.62	0.36	1.64	3.21E-10	2.06E-05	0.0196		28.73
2	12		25.81	9.19	16.62	0.36	1.64	3.21E-10	2.06E-05	0.0196		28.73
3	18		25.81	9.19	16.62	0.36	1.64	3.21E-10	2.06E-05	0.0196		28.73
4	24		25.82	9.19	16.62	0.36	1.64	3.21E-10	2.06E-05	0.0196		28.74
5	30		25.82	9.19	16.63	0.36	1.64	3.21E-10	2.06E-05	0.0196		28.74
6	36		25.82	9.20	16.63	0.36	1.64	3.21E-10	2.06E-05	0.0196		28.74
7	42		25.83	9.20	16.63	0.36	1.64	3.21E-10	2.06E-05	0.0196		28.75
8	48		25.83	9.20	16.63	0.36	1.64	3.21E-10	2.06E-05	0.0196		28.75
9	54		25.83	9.20	16.63	0.36	1.64	3.21E-10	2.06E-05	0.0196		28.76
10	60		25.84	9.20	16.63	0.36	1.64	3.21E-10	2.06E-05	0.0196		28.76
11	66		25.84	9.20	16.63	0.36	1.64	3.21E-10	2.06E-05	0.0196		28.76
12	72		25.84	9.21	16.63	0.36	1.64	3.21E-10	2.06E-05	0.0196		28.77
13	78		25.84	9.21	16.64	0.36	1.64	3.21E-10	2.06E-05	0.0196		28.77
14	84		25.85	9.21	16.64	0.36	1.64	3.21E-10	2.06E-05	0.0196		28.77
15	90		25.85	9.21	16.64	0.36	1.64	3.21E-10	2.06E-05	0.0196		28.78
16	96		25.85	9.21	16.64	0.36	1.64	3.21E-10	2.07E-05	0.0196		28.78
17	102		25.86	9.21	16.64	0.36	1.64	3.21E-10	2.07E-05	0.0196		28.79
18	108		25.86	9.22	16.64	0.36	1.64	3.21E-10	2.07E-05	0.0196		28.79
19	114		25.86	9.22	16.64	0.36	1.64	3.21E-10	2.07E-05	0.0196		28.79
20	120		25.87	9.22	16.65	0.36	1.64	3.21E-10	2.07E-05	0.0197		28.80
21	126		25.87	9.22	16.65	0.36	1.64	3.21E-10	2.07E-05	0.0197		28.80
22	132		25.87	9.22	16.65	0.36	1.64	3.21E-10	2.07E-05	0.0197		28.81
23	138		25.87	9.22	16.65	0.36	1.64	3.21E-10	2.07E-05	0.0197		28.81
24	144		25.88	9.23	16.65	0.36	1.64	3.21E-10	2.07E-05	0.0197		28.81
25	150		25.88	9.23	16.65	0.36	1.64	3.21E-10	2.07E-05	0.0197		28.82

Table 6. Evaluation of an External Axial Flaw for Fatigue Crack Growth Along Path 1 (Cont'd) .

AXIAL CRACK GROWTH FOR AXIAL FLAW (IN-AIR) - AUSTENITIC MATERIAL

Basis: $\Delta a = \Delta N * C_o(\Delta KI)^n$ $\Delta N =$ 6 fatigue cycles / year Sy = 42.5 ksi

Operating Time (yr.)	Cycle	a (in.)	NU1 KI(a)max (ksi√in)	NU2 KI(a)min (ksi√in)	ΔKI (ksi√in)	R	S	C_o	Δa (in.)	r_y	a_e	NU1 KI(a_e)max (ksi√in)
0	0		29.61	9.57	20.03	0.32	1.58	3.10E-10	3.67E-05	0.0257		33.12
1	6		29.61	9.58	20.04	0.32	1.58	3.10E-10	3.67E-05	0.0258		33.12
2	12		29.62	9.58	20.04	0.32	1.58	3.10E-10	3.68E-05	0.0258		33.13
3	18		29.62	9.58	20.04	0.32	1.58	3.10E-10	3.68E-05	0.0258		33.13
4	24		29.63	9.58	20.05	0.32	1.58	3.10E-10	3.68E-05	0.0258		33.14
5	30		29.63	9.58	20.05	0.32	1.58	3.10E-10	3.68E-05	0.0258		33.15
6	36		29.64	9.59	20.05	0.32	1.58	3.10E-10	3.68E-05	0.0258		33.15
7	42		29.65	9.59	20.06	0.32	1.58	3.10E-10	3.69E-05	0.0258		33.16
8	48		29.65	9.59	20.06	0.32	1.58	3.10E-10	3.69E-05	0.0258		33.16
9	54		29.66	9.59	20.07	0.32	1.58	3.10E-10	3.69E-05	0.0258		33.17
10	60		29.66	9.59	20.07	0.32	1.58	3.10E-10	3.69E-05	0.0258		33.18
11	66		29.67	9.59	20.07	0.32	1.58	3.10E-10	3.70E-05	0.0258		33.18
12	72		29.67	9.60	20.08	0.32	1.58	3.10E-10	3.70E-05	0.0259		33.19
13	78		29.68	9.60	20.08	0.32	1.58	3.10E-10	3.70E-05	0.0259		33.19
14	84		29.68	9.60	20.08	0.32	1.58	3.10E-10	3.70E-05	0.0259		33.20
15	90		29.69	9.60	20.09	0.32	1.58	3 10E-10	3.70E-05	0.0259		33.21
16	96		29.69	9.60	20.09	0.32	1.58	3.10E-10	3.71E-05	0.0259		33.21
17	102		29.70	9.60	20.09	0.32	1.58	3.10E-10	3.71E-05	0.0259		33.22
18	108		29.70	9.61	20.10	0.32	1.58	3.10E-10	3.71E-05	0.0259		33.22
19	114		29.71	9.61	20.10	0.32	1.58	3.10E-10	3.71E-05	0.0259		33.23
20	120		29.71	9.61	20.10	0.32	1.58	3.10E-10	3.72E-05	0.0259		33.24
21	126		29.72	9.61	20.11	0.32	1.58	3.10E-10	3.72E-05	0.0259		33.24
22	132		29.73	9.61	20.11	0.32	1.58	3.10E-10	3.72E-05	0.0260		33.25
23	138		29.73	9.62	20.11	0.32	1.58	3.10E-10	3.72E-05	0.0260		33.25
24	144		29.74	9.62	20.12	0.32	1.58	3.10E-10	3.72E-05	0.0260		33.26
25	150		29.74	9.62	20.12	0.32	1.58	3.10E-10	3.73E-05	0.0260		33.27

Table 7. Evaluation of a Continuous Cylindrical Surface Crack for Fatigue Crack Growth Along Path 2

INPUT DATA

Geometry:	Plate thickness,	t =	1.143	in.
Flaw Size:	Flaw depth,	a = [ ]		in.
		a/t = [ ]		
Environment:	Temperature,	T =	600	F

Table 7. Evaluation of a Continuous Cylindrical Surface Crack for Fatigue Crack Growth Along Path 2 (Cont'd)

STRESS INTENSITY FACTOR FOR CYLINDRICAL FLAW IN WELD

Basis: Analysis of Flaws, 1995 ASME Code, Section XI, Appendix A (Ref. 16)

$$KI = [A_0 G_0 + A_1 G_1 + A_2 G_2 + A_3 G_3] \sqrt{(\pi a/Q)}$$

where $Q = 1 + 4.593*(a/l)^{1.65} - q_y$

and $q_y = [(A_0 G_0 + A_1 G_1 + A_2 G_2 + A_3 G_3) / \sigma_{ys}]^2 / 6$

For a/l = 0.0 (continuous flaw)
a/t <= 0.1

Go = 1.1945
G_1 = 0.7732
G_2 = 0.5996
G_3 = 0.5012

Stresses are described by a third order polynomial fit over the flaw depth,

$$S(x) = A_0 + A_1(x/a) + A_2(x/a)^2 + A_3(x/a)^3$$

Radial Stresses in Weld:

Wall Position x	Residual Stress in Weld	Normal/Upset Cond. Stresses [6]		Total Stresses at Operation	
		Cooldown	Shutdown	Cooldown	Shutdown
(in.)	(ksi)	(ksi)	(ksi)	(ksi)	(ksi)
0.000					
0.223					
0.446					
0.670					
0.893					

Stress Coefficients: (a = 0.100 in.)

Stress Coeff.	Normal/Upset Loading Conditions	
	NU1	NU2
	(ksi)	(ksi)
A_0		
A_1		
A_2		
A_3		

Table 7. Evaluation of a Continuous Cylindrical Surface Crack for Fatigue Crack Growth Along Path 2 (Cont'd)

CRACK GROWTH FOR CYLINDRICAL FLAW (IN-AIR) - AUSTENITIC MATERIAL

Basis: $\Delta a = \Delta N * C_o(\Delta KI)^n$ $\Delta N =$ 6 cycles/year Sy = 69.0 ksi

Operating Time (yr.)	Cycle	a (in.)	Q	NU1 KI(a)max (ksi√in)	NU2 KI(a)min (ksi√in)	ΔKI (ksi√in)	R	S	C_o	Δa (in.)	q_y	$Q(a_e)$	$KI(a_e)max$ (ksi√in)
0	0		1.000	39.62	25.00	14.63	0.63	2.14	4.18E-10	1.76E-05	0.175	0.825	43.62
1	6		1.000	39.63	25.00	14.63	0.63	2.14	4.18E-10	1.76E-05	0.175	0.825	43.63
2	12		1.000	39.63	25.00	14.63	0.63	2.14	4.18E-10	1.76E-05	0.175	0.825	43.63
3	18		1.000	39.64	25.01	14.63	0.63	2.14	4.18E-10	1.76E-05	0.175	0.825	43.64
4	24		1.000	39.64	25.01	14.63	0.63	2.14	4.18E-10	1.76E-05	0.175	0.825	43.64
5	30		1.000	39.64	25.01	14.63	0.63	2.14	4.18E-10	1.76E-05	0.175	0.825	43.64
6	36		1.000	39.65	25.01	14.63	0.63	2.14	4.18E-10	1.76E-05	0.175	0.825	43.65
7	42		1.000	39.65	25.01	14.63	0.63	2.14	4.18E-10	1.76E-05	0.175	0.825	43.65
8	48		1.000	39.65	25.02	14.64	0.63	2.14	4.18E-10	1.76E-05	0.175	0.825	43.65
9	54		1.000	39.66	25.02	14.64	0.63	2.14	4.18E-10	1.76E-05	0.175	0.825	43.66
10	60		1.000	39.66	25.02	14.64	0.63	2.14	4.18E-10	1.76E-05	0.175	0.825	43.66
11	66		1.000	39.66	25.02	14.64	0.63	2.14	4.18E-10	1.76E-05	0.175	0.825	43.67
12	72		1.000	39.67	25.03	14.64	0.63	2.14	4.18E-10	1.76E-05	0.175	0.825	43.67
13	78		1.000	39.67	25.03	14.64	0.63	2.14	4.18E-10	1.76E-05	0.175	0.825	43.67
14	84		1.000	39.67	25.03	14.64	0.63	2.14	4.18E-10	1.76E-05	0.175	0.825	43.68
15	90		1.000	39.68	25.03	14.65	0.63	2.14	4.18E-10	1.76E-05	0.175	0.825	43.68
16	96		1.000	39.68	25.03	14.65	0.63	2.14	4.18E-10	1.76E-05	0.175	0.825	43.69
17	102		1.000	39.68	25.04	14.65	0.63	2.14	4.18E-10	1.76E-05	0.175	0.825	43.69
18	108		1.000	39.69	25.04	14.65	0.63	2.14	4.18E-10	1.76E-05	0.175	0.825	43.69
19	114		1.000	39.69	25.04	14.65	0.63	2.14	4.18E-10	1.76E-05	0.175	0.825	43.70
20	120		1.000	39.69	25.04	14.65	0.63	2.14	4.18E-10	1.77E-05	0.175	0.825	43.70
21	126		1.000	39.70	25.04	14.65	0.63	2.14	4.18E-10	1.77E-05	0.175	0.825	43.70
22	132		1.000	39.70	25.05	14.65	0.63	2.14	4.18E-10	1.77E-05	0.175	0.825	43.71
23	138		1.000	39.70	25.05	14.66	0.63	2.14	4.18E-10	1.77E-05	0.175	0.825	43.71
24	144		1.000	39.71	25.05	14.66	0.63	2.14	4.18E-10	1.77E-05	0.175	0.825	43.72
25	150		1.000	39.71	25.05	14.66	0.63	2.14	4.18E-10	1.77E-05	0.175	0.825	43.72

Table 7. Evaluation of a Continuous Cylindrical Surface Crack for Fatigue Crack Growth Along Path 2 (Cont'd)

STRESS INTENSITY FACTOR FOR CYLINDRICAL FLAW IN HEAD

Basis: Analysis of Flaws, 1995 ASME Code, Section XI, Appendix A (Ref. 16)

$$KI = [\, A_0 G_0 + A_1 G_1 + A_2 G_2 + A_3 G_3 \,] \sqrt{(\pi a/Q)}$$

where $Q = 1 + 4.593*(a/l)^{\wedge}1.65 - q_y$

and $q_y = [\, (A_0 G_0 + A_1 G_1 + A_2 G_2 + A_3 G_3) / \sigma_{ys} \,]^2 / 6$

For a/l = 0.0 (continuous flaw)
a/t <= 0.1

Go = 1.1945
G_1 = 0.7732
G_2 = 0.5996
G_3 = 0.5012

Stresses are described by a third order polynomial fit over the flaw depth,

$$S(x) = A_0 + A_1(x/a) + A_2(x/a)^2 + A_3(x/a)^3$$

Radial Stresses in Weld:

Wall Position x	Residual Stress in Weld	Normal/Upset Cond. Stresses [6]		Total Stresses at Operation	
		Cooldown	Shutdown	Cooldown	Shutdown
(in.)	(ksi)	(ksi)	(ksi)	(ksi)	(ksi)
0.000					
0.223					
0.446					
0.670					
0.893					

Stress Coefficients: (a = 0.100 in.)

Stress Coeff.	Normal/Upset Loading Conditions	
	NU1	NU2
	(ksi)	(ksi)
A_0		
A_1		
A_2		
A_3		

Table 7. Evaluation of a Continuous Cylindrical Surface Crack for Fatigue Crack Growth Along Path 2 (Cont'd)

CRACK GROWTH FOR CYLINDRICAL FLAW (IN-AIR) - FERRITIC MATERIAL

Basis: $\Delta a = \Delta N * C_o(\Delta KI)^n$ $\Delta N =$ 6 cycles/year Sy = 57.6 ksi

Operating Time (yr.)	Cycle	a (in.)	Q	NU1 KI(a)max (ksi√in)	NU2 KI(a)min (ksi√in)	ΔKI (ksi√in)	R	S	C_o	Δa (in.)	q_y	$Q(a_e)$	$KI(a_e)max$ (ksi√in)
0	0		1.000	38.08	23.46	14.63	0.62	2.09	4.16E-10	9.43E-06	0.232	0.768	43.45
1	6		1.000	38.08	23.46	14.63	0.62	2.09	4.16E-10	9.44E-06	0.232	0.768	43.45
2	12		1.000	38.09	23.46	14.63	0.62	2.09	4.16E-10	9.44E-06	0.232	0.768	43.46
3	18		1.000	38.09	23.46	14.63	0.62	2.09	4.16E-10	9.44E-06	0.232	0.768	43.46
4	24		1.000	38.09	23.46	14.63	0.62	2.09	4.16E-10	9.44E-06	0.232	0.768	43.46
5	30		1.000	38.09	23.46	14.63	0.62	2.09	4.16E-10	9.44E-06	0.232	0.768	43.46
6	36		1.000	38.09	23.46	14.63	0.62	2.09	4.16E-10	9.44E-06	0.232	0.768	43.46
7	42		1.000	38.09	23.46	14.63	0.62	2.09	4.16E-10	9.44E-06	0.232	0.768	43.47
8	48		1.000	38.10	23.46	14.63	0.62	2.09	4.16E-10	9.44E-06	0.232	0.768	43.47
9	54		1.000	38.10	23.47	14.63	0.62	2.09	4.16E-10	9.45E-06	0.232	0.768	43.47
10	60		1.000	38.10	23.47	14.63	0.62	2.09	4.16E-10	9.45E-06	0.232	0.768	43.47
11	66		1.000	38.10	23.47	14.63	0.62	2.09	4.16E-10	9 45E-06	0.232	0.768	43.47
12	72		1.000	38.10	23.47	14.63	0.62	2.09	4.16E-10	9.45E-06	0.232	0.768	43.48
13	78		1.000	38.11	23.47	14.63	0 62	2.09	4.16E-10	9.45E-06	0.232	0.768	43.48
14	84		1.000	38.11	23.47	14.64	0.62	2.09	4.16E-10	9.45E-06	0 232	0.768	43.48
15	90		1.000	38.11	23.47	14.64	0.62	2.09	4.16E-10	9.45E-06	0.232	0.768	43.48
16	96		1.000	38.11	23.47	14.64	0.62	2.09	4.16E-10	9.46E-06	0.232	0.768	43.48
17	102		1.000	38.11	23.47	14.64	0.62	2.09	4.16E-10	9.46E-06	0.232	0.768	43.49
18	108		1.000	38.11	23.48	14.64	0.62	2.09	4.16E-10	9.46E-06	0.232	0.768	43.49
19	114		1.000	38.12	23.48	14.64	0.62	2.09	4.16E-10	9.46E-06	0.232	0.768	43.49
20	120		1.000	38.12	23.48	14.64	0.62	2.09	4.16E-10	9.46E-06	0.232	0.768	43.49
21	126		1.000	38.12	23.48	14.64	0.62	2.09	4.16E-10	9.46E-06	0.232	0.768	43.49
22	132		1.000	38.12	23.48	14.64	0.62	2.09	4.16E-10	9.46E-06	0.232	0.768	43.50
23	138		1.000	38.12	23.48	14.64	0.62	2.09	4.16E-10	9.47E-06	0.232	0.768	43.50
24	144		1.000	38.12	23.48	14.64	0.62	2.09	4.16E-10	9.47E-06	0.232	0.768	43.50
25	150		1.000	38.13	23.48	14.64	0.62	2.09	4.16E-10	9.47E-06	0.232	0.768	43.50

9.0 SUMMARY OF RESULTS

The flaw evaluation results for 25 years of fatigue crack growth are as follows.

9.1 Propagation of a Continuous External Circumferential Flaw Along Path 1

a) Fatigue crack growth analysis:

Initial flaw size,	a_i = [ ] in.
Final flaw size,	a_f < [ ] in.
Stress intensity factor at final flaw size,	$K_I(a_{ef})$ < 0 ksi√in
Fracture toughness	K_{Ia} = 200 ksi√in
Fracture toughness margin,	K_{Ia} / K_I > √10

b) Limit load analysis:

Limit load,		P_O = [ ] lbs
Applied loads:	normal/upset,	P = [ ] lbs
	emergency/faulted,	P = [ ] lbs
Limit load margins:	normal/upset,	P_O / P = 9.44 > 3.0
	emergency/faulted,	P_O / P = 6.67 > 1.5

9.2 Fatigue Crack Growth of a Semi-Circular External Axial Flaw Along Path 1

Initial flaw size, a_i = [ ] in.

Radial Growth

Final flaw size,	a_f < [ ] in.
Stress intensity factor at final flaw size,	$K_I(a_{ef})$ = 28.8 ksi√in
Fracture toughness	K_{Ia} = 200 ksi√in
Fracture toughness margin,	K_{Ia} / K_I = 6.94 > √10

Axial Growth

Final flaw size,	a_f < [ ] in.
Stress intensity factor at final flaw size,	$K_I(a_{ef})$ = 33.3 ksi√in
Fracture toughness	K_{Ia} = 200 ksi√in
Fracture toughness margin,	K_{Ia} / K_I = 6.01 > √10

9.3 Fatigue Crack Growth of a Continuous Cylindrical Flaw Along Path 2

Initial flaw size,	a_i = [ ] in.
Final flaw size,	a_f < [ ] in.
Stress intensity factor at final flaw size,	$K_I(a_{ef})$ = 43.7 ksi√in
Fracture toughness	K_{Ia} = 200 ksi√in
Fracture toughness margin,	K_{Ia} / K_I = 4.58 > √10

10.0 CONCLUSION

The results of the analysis demonstrate that the [ ] inch weld anomaly is acceptable for a 25 year design life of the CRDM ID temper bead weld repair. Significant fracture toughness margins have been demonstrated for both of the flaw propagation paths considered in the analysis. The minimum fracture toughness margins for flaw propagation Paths 1 and 2 have been shown to be 6.01 and 4.58, respectively, as compared to the required margins of $\sqrt{10}$ for normal/upset conditions and $\sqrt{2}$ for emergency/faulted conditions per Section XI, IWB-3612 (Reference 3). Fatigue crack growth is minimal. The maximum final flaw size is less than 0.101 inch (considering both flaw propagation paths). A limit load analysis was also performed considering the ductile Alloy 600 and Alloy [ ] materials along flaw propagation Path 1. The analysis showed limit load margins of 9.44 for normal/upset conditions and 6.67 for emergency/faulted conditions, as compared to the required margins of 3.0 and 1.5, respectively, per Section XI, IWB-3642 (Reference 3).

11.0 REFERENCES

1. Framatome ANP Drawing 02-5021508E-2, "CRDM Nozzle ID Temper Bead Weld Repair, ANO-1."

2. Framatome ANP Document 51-5021517-01, "ANO-1 CRDM Nozzle ID Ambient Temperature Temper Bead Weld Repair Requirements," November 2002.

3. ASME Boiler and Pressure Vessel Code, Section XI, Rules for Inservice Inspection of Nuclear Power Plant Components, 1992 Edition with No Addenda.

4. BAW-10046A, Rev. 2, "Methods of Compliance With Fracture Toughness and Operational Requirements of 10 CFR 50, Appendix G," B&W Owners Group Materials Committee Topical Report, June 1986.

5. Framatome ANP Document 38-1290261-00, ANO Design Input Record No. 2001-0230-020-02, dated 11/6/2002 forwarding Dominion Engineering Stress Calculations for IDTB Weld Repair.

6. Framatome ANP Document 32-5012424-10, "CRDM Temperbead Bore Weld Analysis," November 2002.

7. ASME Section II, Part C, "Specification for Welding Rods, Electrodes, and Filler Metals," 1999 Addenda.

8. Framatome ANP Document 38-1288355-00, "Flaw Acceptance Criteria."

9. ASME Boiler and Pressure Vessel Code, Section III, Rules for Construction of Nuclear Power Plant Components, Division 1 - Appendices, 1989 Edition with No Addenda.

10. I.S. Raju and J.C. Newman Jr., "Stress Intensity Factors for Internal and External Surface Cracks in Cylindrical Vessels," Transactions of the ASME, Journal of Pressure Vessel Technology, pp. 293-298, Vol. 104, November 1982.

11. T.L. Anderson, Fracture Mechanics: Fundamentals and Applications, CRC Press, 1991.

12. W.J. Mills, "Fracture Toughness of Two Ni-Fe-Cr Alloys," Hanford Engineering Development Laboratory Document HEDL-SA-3309, April 1985.

13. C.B. Buchalet and W.H. Bamford, "Stress Intensity Factor Solutions for Continuous Surface Flaws in Reactor Pressure Vessels," Mechanics of Crack Growth, ASTM STP 590, American Society for Testing and Materials, 1976, pp. 385-402.

14. EPRI Topical Report, EPRI NP-1931, "An Engineering Approach for Elastic-Plastic Fracture Analysis," Research Project 1237-1, prepared by V. Kumar et al of General Electric Company, July 1981.

15. General Electric Report, SRD-82-048, "Estimation Technique for the Prediction of Elastic-Plastic Fracture of Structural Components of Nuclear Systems," by V. Kumar et al, Contract RP1237-1, Combined Fifth and Sixth Semi-Annual Report, March 1982.

16. ASME Boiler and Pressure Vessel Code, Section XI, Rules for Inservice Inspection of Nuclear Power Plant Components, Appendix A, Analysis of Flaws, 1995 Edition with No Addenda (used for updated stress intensity factor solution).

17. Framatome ANP Document 32-5012403-00, "Oc-3 CRDM Nozzle Circumferential Flaw Evaluations," April 2001.

18. EPRI Topical Report, EPRI NP-3607, "Advances in Elastic-Plastic Fracture Analysis," Research Project 1237-1, prepared by V. Kumar et al of General Electric Company, August 1984.

19. Framatome ANP Document 18-1173987-03, "RCS Functional Specification for ANO-1."

20. Letter from Entergy for Reactor Trip Transients, November 8, 2002 (attached as Appendix B).

Appendix A

Certification Document

ANO-1 CRDM NOZZLE IDTB WELD ANOMALY FLAW EVALUATIONS

SHEET 1 OF 1

I certify that the flaw evaluations contained in this calculation package are evidence that the CRDM nozzle repair, as defined by Framatome ANP drawing 02-5021508E-2, meets the fracture mechanics requirements identified in Framatome ANP Document 51-5021517-01 and the ASME Boiler and Pressure Vessel Code, Section XI, 1992 Edition with no addenda, for the design transients provided in Framatome ANP Document 18-1173987-03.

Exception:

The rod withdrawal transient, identified as Transient No. 11 in the functional specification for the reactor coolant system at ANO-1 (Framatome ANP Document 18-1173987-03), is analyzed as an emergency condition transient since ANO-1 has not experienced any rod withdrawal transient transients during its plant life and the likelihood of even a single future occurrence is remote. It is even more unlikely that a CRDM nozzle would experience 25 cycles of this transient, which is a requirement for classification as an emergency event.

Attested to this date: November 8, 2002

By: N/A

Douglas E. Killian
Framatome ANP, Inc.
Nuclear Engineering Business Unit
Lynchburg, Virginia

License No. 15308
Virginia Board for Architects,
Professional Engineers,
Land Surveyors,
Certified Interior Designers,
and Landscape Architects

Appendix B

Letter from Entergy for Reactor Trip Transients

32-5021539-01

ARKANSAS NUCLEAR ONE
GENERATION SUPPORT BUILDING
1448 S. R. 333
RUSSELLVILLE, AR 72801

FAX COVERLETTER

DATE 11/8/02

TO Steve Son

COMPANY NAME Pressure - ANP

CITY, STATE

FAX NUMBER VERIFY

NUMBER OF PAGES INCLUDING COVER

FROM Raymond To

COMPANY NAME Entergy

DEPARTMENT

FAX NUMBER (501) 858-4955 VERIFY (501) 858-4302

COMMENTS See attached 1 page

TO BE COMPLETED BY SENDER
AFTER TRANSMISSION IS COMPLETE, PLEASE
RETURN BY MAIL____ DISCARD____ CALL FOR PICK-UP
PHONE NUMBER_____

32-5021539-01

Steve:

Based on a review performed by our System Engineering, as documented in our ER-ANO-2001-0230-024, ANO-1 has not had a "high pressure, rod withdrawal accident" as described in transient No. 11 of RCS Functional Specification 18-1173987-03. See below for details.

++

From: MEANS, BRACY E
Sent: Friday, November 08, 2002 11:20 AM
To: TO, RAYMOND M; BAUMAN, DAVID N; CHISUM, MICHAEL R; DAIBER, BRYAN J; CHADBOURN, HARMON C; GRAY, BRIAN C; LEWIS, RAYMOND S
Subject: Reactor Trip Transients

Raymond,

The RCS Functional Specification Transient 11 (Rod Withdrawal Accident (upset condition) defines this condition as follows:
"The rod withdrawal accident occurs when one group of control rods is accidentally withdrawn from the core at the maximum rate when the reactor is operating at a low power. This transient is assumed to occur when the reactor is operating at 15% power. This causes a rapid rise in power and a reactor trip."
In an effort to facilitate transient cycle counting, FTI performed a review of the functional specification transients and consolidated the above transient in what is currently tracked as Transient #19. This FTI report has been filed as Engineering Report 95R-1015-01 and is FTI document number 51-1235146-01. In the FTI report, ANO historical transients though the year 1995 were reviewed and consolidated to reflect the current transient cycle recording document reflected in Procedure 1010.010. The transient cycle log procedure 1010.010 currently records reactor trip transients for the following conditions:

- Transient 17 - Reactor Trips with loss of RC flow. There have been 10 recorded transients in this category.
- Transient 18 - Reactor Trips with Post Overcooling. There have been 0 transients recorded in this category. The 5/18/1996 trip did not meet the overcooling requirements to be recorded in this category. It was captured in transient 19.
- Transient 19 - All Other Reactor Trips. There have been 96 recorded transients in this category through December 31, 2001. There were two RPS high pressure trips recorded. These high pressure trips did not cause a Pressurizer Code Safety valve relief with set point of 2500 psi.

The control room logs were reviewed in Autolog as well as PCRS with the plant computer data to assess related trips that may have met the criteria for Functional Specification Transient #11. **Based on this level of review, it can be stated that ANO-1 has not experienced any of the Functional Specification transient #11 events since commercial operation.** Please be advised that the transients associated with plant performance for the 2002 operating year have not been finalized. However, it is certain that none of the Functional Specification Transient #11 conditions have been experienced for ANO-1 for this year. Please advise if there are any clarifications required for the data provided herewith or if any additional input or research is desired.

Bracy

++

Raymond M. To 11/8/02

Entergy

ANO-Design Engineering Structural Group